~~Western Indian Ocean bottom water temperature calibration – are benthic foraminifera Mg/Ca ratios a reliable palaeothermometry proxy?~~Persistent contamination in benthic foraminifera-based Mg/Ca thermometry using standard cleaning methods

Viktoria Larsson[1] and Simon Jung[1]

[1] School of Geosciences, University of Edinburgh, Edinburgh, EH9 3FE, United Kingdom

Correspondence to: Viktoria Larsson (viktorialarsson3@gmail.com)

Abstract: Mg/Ca ratios measured in benthic foraminifera have been explored as a potential palaeothermometry proxy for bottom water temperatures (BWT). Mg/Ca-BWT calibrations from the Indian Ocean are rare and comprise conflicting results. Inconsistencies between studies suggest that calibrations may need to be region specific. The aim of this study was to develop species-specific benthic foraminifera (*Uvigerina peregrina, Cibicidoides wuellerstorfi* and *Cibicidoides mundulus*) based Mg/Ca – BWT calibrations in the tropical western Indian Ocean and to optimise the chemical cleaning procedure by Barker et al. (2003) applied to samples analysed in this study. ~~Testing variations of existing analytical protocols, aimed at optimising cleaning of the foraminifera while avoiding sample loss in the process, entailed that a previously established protocol by Barker et al. (2003) was the most suitable for our study.~~ The majority of samples of *C.~~ibicidoides~~ mundulus* and *U.~~vigerina~~ peregrina*, however, remained contaminated, rendering those data unusable for Mg/Ca core-top calibrations. Only Mg/Ca ratios in *C.~~ibicidoides~~ wuellerstorfi* allowed a tentative Mg/Ca - BWT calibration with the relationship being: $\mathrm{Mg/Ca} = 0.19 \pm 0.02 * \mathrm{BWT} + 1.07 \pm 0.03, r^2 = 0.87$ and n = 4). While this result differs to some degree from previous studies it principally suggests that existing core-top calibrations from the wider Indian Ocean can be applied to core-tops in the western Indian Ocean. The agreement of Mg/Ca ratios at lower temperatures in *C. ~~Cibicidoides~~ wuellerstorfi*, *C.~~ibicidoides~~ mundulus* and *U.~~vigerina~~ peregrina* with Mg/Ca ratios reported for these species at low temperatures in other studies supports this conclusion. The clear difference in contamination, between *Cibicidoides spp*. and *U. peregrina* despite using the same cleaning procedure, supports the findings of previous studies that suggest different rigour might be required for different species. Many other uncertainties surrounding the Mg/Ca proxy exist and more calibration studies are required to improve this method.

1. Introduction

~~The global thermohaline circulation is crucial for distributing heat, nutrients, oxygen and salinity and it partially controls the oceanic carbon uptake (Blunier et al., 1998; Clark et al., 2002). Specifically, the re-/distribution of heat is an important driver of climate change, with Antarctic Intermediate Water (AAIW), Antarctic Bottom Water (AABW) and North Atlantic Deep Water (NADW) representing crucial water masses. Palaeoceanographic reconstructions have greatly improved our understanding of the sensitivity and of changes of the thermohaline circulation. On glacial-interglacial time scales for example NADW and AABW importance seems to have alternated between NADW being more prominent during interglacials and AABW during glacials (Duplessy et al, 1988, Curry et al., 1988, Sarnthein et al., 1994). These water mass reorganisations had largescale implications on global climate (Blunier et al., 1998).~~

There are a range of proxies measured in foraminifera used to reconstruct changes in seawater properties through time. Stable oxygen isotopes ($\delta^{18}O$) have been widely applied to identify changes in water column properties (Kroopnick, 1985; Lynch-Stieglitz and Fairbanks, 1994). Straightforward interpretation, however, is hampered due to stable oxygen isotopes reflecting more than one environmental factor, i.e. ambient temperatures and seawater $\delta^{18}O$ with the latter being controlled by global ice volume and the evaporation-precipitation balance in the water mass source region (Emiliani, 1955; Shackleton, 1974). In order to improve the use of $\delta^{18}O$ values, independent temperature proxies have been developed (Elderfield and Ganssen, 2000; Lea et al., 1999; Nuernberg, 1995; Nuernberg et al., 1996). Mg/Ca based temperature estimates in planktic foraminifera for example are widely used as a proxy for sea surface temperature (SST, Barker, 2005). The use of Mg/Ca ratios in benthic foraminifera for reconstructions of bottom water temperatures (BWT) is being explored (Rosenthal et al. 1997; Elderfield et al., 2006) although there is no widely accepted method as yet. Mg/Ca based BWT reconstructions, used in combination with other proxies such as $\delta^{18}O$, are potentially crucial for our understanding of reorganisations of deep and bottom waters associated with for example past glacial/interglacial transitions (Duplessy et al, 1988; Curry et al., 1988; Sarnthein et al., 1994). In order to assess the robustness of the Mg/Ca based thermometry in deep/intermediate water based on benthic foraminifera, we present (Mg/Ca – based BWT calibrations derived from the benthic foraminiferal species *Uvigerina peregrina (U. peregrina)*, *Cibicidoides wuellerstorfi (C. wuellerstorfi)* and *Cibicidoides mundulus (C. mundulus)* using core top samples from the western tropical Indian Ocean and compare those with previously published calibrations from the Indian Ocean (Elderfield et al., 2006; Healey et al., 2008). We also assess the usefulness of adaptations of cleaning procedures.

~~There are a range of proxies measured in foraminifera used to reconstruct changes in seawater properties through time. Stable oxygen isotopes ($\delta^{18}O$) have been widely applied to identify changes in water column properties (Kroopnick, 1985; Lynch-Stieglitz and Fairbanks, 1994). Straightforward interpretation, however, is hampered due to stable oxygen isotopes reflecting more than one environmental factor, i.e. ambient temperatures and seawater $\delta^{18}O$ with the latter being controlled by global ice volume and evaporation-precipitation in the water mass source region (Emiliani, 1955; Shackleton, 1974). In order to improve the use of stable oxygen isotopes, independent temperature proxies have been developed (Elderfield and Ganssen, 2000; Lea et al., 1999; Nuernberg, 1995; Nuernberg et al., 1996). Mg/Ca based temperature estimates in planktic foraminifera for example are widely used as a proxy for sea surface temperature (SST, Barker, 2005). The use of Mg/Ca ratios in benthic foraminifera for reconstructions of bottom water temperature (BWT) is being explored (Rosenthal et al. 1997; Elderfield et al., 2006) although a uniformly adopted method is still being developed.~~

1.1. Mg/Ca ratios - a proxy for temperature

Foraminifera form calcite tests, which is a lattice composed of calcium carbonate. During ~~the~~ carbonate formation~~rmation of tests of foraminifera~~, divalent ions of trace elements such as Mg^{2+} ~~are~~ substitute Ca^{2+} ~~also~~ ~~incorporated into~~in the calcite lattice

(Erez, 2003). Resulting Mg/Ca ratios in benthic foraminifera depend on the Mg/Ca ratio of ambient ~~sea~~water and elemental partitioning during calcite precipitation with the latter depending on ambient water temperature (Elderfield et al., 1996; Gussone et al. 2016). On glacial-interglacial timescales Mg/Ca ratios in seawater can be considered constant due to long residence times for Ca and Mg (~10^6 and 10^7 years, respectively). Hence, Mg/Ca ratios can be used to reconstruct BWT. Existing core-top calibrations show a positive correlation between Mg/Ca ratios in a number of species of benthic ~~hyaline low magnesium calcite~~ foraminifera and modern BWTs (Martin and Lea, 2002; Elmore et al., 2015). Temperature appears to be the dominant environmental factor controlling incorporation of Mg in tests of ~~in~~ some species of *Cibicidoides spp.* (Rosenthal et al., 1997) but other factors including carbonate ion saturation might also ~~have an effect~~affect Mg inclusion (Elderfield et al., 2006; Yu and Elderfield, 2008). There is discussion ~~on~~ surrounding the importance of various factors controlling Mg/Ca incorporation in benthic foraminifera, with e.g. Yu and Elderfield (2008) suggesting carbonate ion saturation being dominant whereas Lear et al.'s (2002) work implies only a minor influence. There is also evidence suggesting that the Mg/Ca - temperature relationships and the ~~other controlling factors including~~ carbonate ion effect ~~are spatially~~ varies between different ocean basins and depositional environments ~~ying~~ (Bryan and Marchitto, 2008).

1.2. Mg/Ca analysis – a brief summary

The chemical cleaning procedure is a critical step essential for accurate determination of Mg/Ca ratios in foraminifera (Barker et al., 2003) due to the generally low Mg/Ca concentration ratios, entailing the need to remove Mg containing contaminants (Barker et al., 2003; Marr et al., 2013). Concurrently, carbonate dissolution of tests may affect Mg/Ca ratios (Lear et al., 2002) and therefore the aim of a cleaning procedure is to effectively clean tests while minimising sample loss (Barker et al., 2003). Silicate contamination is the most critical contaminant affecting Mg/Ca ratios, followed by Mn-oxide coatings (Barker et al., 2003). The two most widely used cleaning methods are the 'Mg cleaning method' also referred to as the 'oxidative cleaning method' by Barker et al. (2003) based on Boyle and Keigwin (1985), and the 'Cd cleaning method' also referred to as the 'reductive oxidative cleaning method' by Boyle and Keigwin (1985) and Rosenthal et al. (1995, 1997b). Both methods include successive rinses with ultrapure water followed by methanol cleaning, and an oxidative cleaning step to remove silicates. The 'Cd cleaning method' in addition includes a reductive step to remove Mn-oxide coatings. The procedure was originally intended for determination of Cd/Ca ratios (Boyle and Keigwin, 1985) because Cd concentrations in calcite are significantly lower than Mg concentrations and therefore contamination is more critical (Marr et al., 2013). While the more aggressive 'Cd cleaning procedure' is not viewed as needed for accurate Mg/Ca analyses (Barker et al., 2003; Yu et al., 2008), it is still used (Stirpe et al., 2021) amid continued uncertainty surrounding the requirement of additional rigour for accurate Mg/Ca analyses (e.g. Pena et al., 2005; Has~~z~~enfratz et al., 2017). Whilst the additional reductive step is implemented to ensure removal of diagenetic coatings, ~~On the other hand, the additional reductive step~~ it results in an estimated ~15 % lowering of Mg/Ca ratios due to partial preferential dissolution ~~seems to lower Mg/Ca ratios due to partial preferential dissolution~~ of Mg-rich calcite (Barker et al., 2003; Yu et al., 2007). In comparison, if the reductive step is excluded, diagenetic coatings only causes an -estimated ~1% increase ~~causing a significantly larger (~15%) lowering in Mg/Ca ratios than the increase~~ in Mg/Ca ratios ~~due to diagenetic coatings~~ (Barker et al., 2003; Yu et al. 2007) rendering the reductive step not required in most cases. Therefore, the majority ~~(only ~1%; Barker et al. (2003) and Yu et al. (2007)).~~ of ~~Most~~ studies ~~using Mg/Ca ratios in benthic foraminifera~~ have utilised the 'Mg cleaning procedure' (e.g. Elderfield et al., 2006; Elderfield et al., 2010; ~~,~~ Elmore et al., 2015), ~~thereby~~ target~~inging the most important contaminants, i.e.~~ silicate contamination, organic matter, Mn-oxide coatings, and secondary calcification (Barker et al., 2003). Furthermore, rather than analysing multiple whole-shell specimen of foraminifera for analysis by solution in ICP-MS/ICP-OES, Stirpe et al. (2021) used laser ablation ICP-MS measuring Mg/Ca ratios revealing unevenly distributed Mg/Ca ratios between different chambers in *Uvigerina spp.* Also, Branson et al. (2013) analysed tests of two species of planktic foraminifera showing a systematic banding of Mg distribution. Based on these findings, whole-shell analysis by solution remains the most appropriate method of determining bulk or whole specimen calcite Mg/Ca ratios (Stirpe et al., 2021).

1.3. Species specific Mg/Ca – temperature calibrations

~~The e~~Earlie~~rest~~~~Earlier~~ studies ~~developed~~ of Mg/Ca – BWT calibrations~~,~~ used ~~using~~ mixed benthic foraminifera of the same genera, mostly *Cibicidoides spp.* (e.g. Rosenthal et al., 1997). Later work, however, implies a species-specific temperature sensitivity driving the Mg/Ca signal (Lear et al., 2002; see ~~figure~~ Fig. 1 for locations within the Indian Ocean). ~~*Cibicidoides*~~ *C. wuellerstorfi* has~~ve~~ been one of the most widely used benthic species for stable $\delta^{18}O$ and $\delta^{13}C$ reconstructions (e.g. Bell et al., 2014; Bickert and Mackensen, 2003; Duplessy et al., 1988; Jung et al., 2009; Sarnthein et al., 1994). ~~.~~It is advantageous over other benthic species because it is a true epifaunal species (Lutze and Thiel, 1989) and suggested to record bottom water properties~~ (Lutze and Thiel, 1989)~~. However, some core-top studies suggest Mg~~/Ca~~ signatures or incorporation in *C.* ~~*ibicidoides*~~ *wuellerstorfi* is significantly influenced by carbonate ion saturation (Elderfield et al., 2006 - see F~~f~~ig.~~gure~~ 1 for locations within the Indian Ocean; Yu and Elderfield, 2008), limiting its use as a proxy for BWT. In contrast Mg/Ca ratios in shallow endofaunal *Uvigerina spp.* seem to be independent of carbonate ion saturation and *U. peregrina* has therefore been presented as a promising Mg/Ca-based thermometry species (Yu and Elderfield, 2008; Elderfield et al., 2010; Stirpe et al., 2021; Elmore et al., 2015). The inconsistencies between studies remain and factors influencing different species require more attention ~~with Mg/Ca ratios in *Uvigerina peregrina* being useable as a proxy for temperature at intermediate depths <2.4 km, based on calibration data from the southwest Pacific Ocean (Stirpe et al., 2021). Uncertainties remain (Stirpe et al., 2021), however, entailing~~ pointing to the need for more Mg/Ca core-top calibrations in ~~various~~ different depositional environments using more than one species.

~~areas to assess the robustness of the Mg/Ca thermometry in benthic foraminifera.~~

~~In order to help improving our understanding of Mg/Ca based thermometry in deep/intermediate water based on benthic foraminifera, we present benthic foraminiferal (*Uvigerina peregrina*, *Cibicidoides wuellerstorfi* and *Cibicidoides mundulus*) based Mg/Ca – temperature calibrations using core top samples from the western tropical Indian Ocean and compare those with calibrations from the Indian Ocean. We also assess the usefulness of adaptions to cleaning procedures.~~

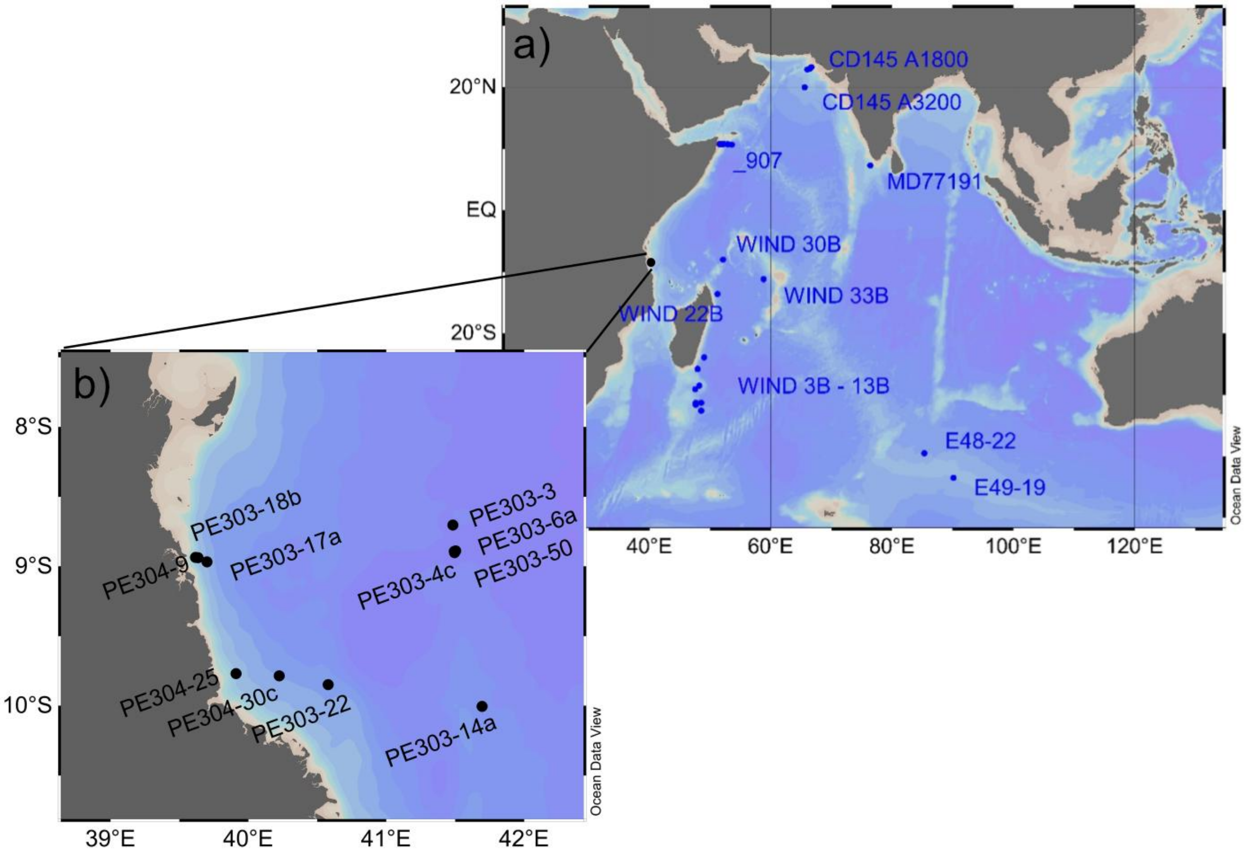

Figure~~.~~ 1. Map showing location of a) existing sediment core-top benthic Mg/Ca – BWT calibrations in the Indian Ocean (blue) and b) the location of cores analysed in this study (black). Map has been produced in Ocean Data View.

2. METHODOLOGY

2.1. Sample location and hydrography

This study is based on a transect of sediment surface samples retrieved from 370 to 3400 m water depth off Tanzania (see Fig. 1 and Table 1). In order to optimise sample quality, only box core or multicorer samples were used (Table 1). The cores have been taken during the Dutch "Indian – Atlantic Exchange (INATEX)" (Brummer and Jung, 2009) and the "Tropical Temperature History during Paleogene Global Warming Events (GLOW)" (Kroon et al., 2010) expeditions. In the modern western Indian Ocean, the water column at our core-top transect is comprised of AABW below 4000 m and Circumpolar Deep Water (CDW) between 2000 and ~3500 m (Fig. 3, You et al., 2000; McCave et al., 2005), the latter itself comprising Lower CDW (LCDW) and Upper (UCDW). NADW and AABW are the main contributors to LCDW, whereas UCDW is a mix of Indian and Pacific common waters (for a summary see Srinivasan (1999)). Above CDW there is a zone influenced by Red Sea Water (RSW) and/or Antarctic Intermediate Water (AAIW), with both water masses extending south- and northwards, respectively, controlling intermediate depth water properties at the location of our core top transect (Fig. 2-3; sensu Talley, 1999; Gründlingh, 1985 and McCave et al., 2005). Based on two nearby CTD profiles (measured during the GLOW expedition, Birch et al., 2013), bottom water temperatures range from 1 to 10˚C (Table 1).

~~This study is based on a transect of sediment surface samples retrieved from 370 to 3400 m water depth off Tanzania (see Figure 1 and Table 1). In order to optimise sample quality, only box core or multicorer samples were used (Table 1). The cores~~

~~have been taken during the “Indian – Atlantic Exchange (INATEX)” (Brummer and Jung, 2009) and the “Tropical Temperature History during Paleogene Global Warming Events (GLOW)” (Kroon et al., 2010) expeditions. In the modern western Indian Ocean, the water column at our core-top transect comprises three bottom to intermediate water masses, i.e. AABW below 4000 m, Circumpolar Deep Water (CDW) between 2000 and ~3500 m (Figure 3, You et al., 2000; McCave et al., 2005). Above CDW there is a zone influenced by Red Sea Water (RSW) and/or Antarctic Intermediate Water (AAIW), with both water masses extending south- and northwards, respectively, controlling intermediate depth water properties at the location of our core top transect (Figure 2-3; sensu Talley, 1999; Gründlingh, 1985 and McCave et al., 2005). Based on a nearby CTD profile, bottom water temperatures at the transect range from 1 to 10˚C (Table 1).~~

Table ~~.~~1. Details of core-top samples of benthic foraminifera analysed in this study

Core	Core type	Latitude (˚W)	Longitude (˚E)	Depth (m)	BWT (˚C)	Species	Size fraction (µm)	Specimens (count)
PE303-3	BC	-8.7034	41.48307	3006	1.74[5]	*C~~ib~~. wuellerstorfi*	250 – 450	15
						Cibicidoides~~ib.~~ sppp~~.~~	250 – 450	9
PE303-4c	BC	-8.89300	41.49298	3179	1.61[5]	*U. ~~vi.~~peregrina~~spp.~~*	150 – 450	8
						C~~ib~~. wuellerstorfi	150 – 450	7
PE303-5	BC	-8.90167	41.49507	3371	1.46[5]	*C~~ib~~ibicidoides~~.~~ spp~~.~~*	150 – 450	12
PE303-6a	BC	-8.88828	41.5038	3323	1.48[5]	*U~~vi~~. peregrina~~spp.~~*	150 – 250	15
						U. peregrina	-250 – 450	8
						C~~ib~~. mundulus	250 – 450	5
						C~~ib~~. wuellerstorfi	150 – 450	19
PE303-14a	BC	-10.00415	41.69455	2560	2.32[2]	*U~~Uvi~~. peregrina~~spp.~~*	250 – >450	6
						Cibicidoides~~ib.~~ spp.	250 – 450	10
PE303-17a	BC	-8.96737	39.70033	1105	5.34[5]	*U~~Uvi~~. peregrina~~spp.~~*	250 – 450	18
PE303-18b	BC	-8.93778	39.63465	490	8.59[5]	*U~~vi~~. peregrina~~spp.~~*	250 – 450	44
						C~~Cib~~. w~~W~~uellerstorfi	250 – 450	8
						C~~ib~~. mundulus	>450	4
PE303-22	BC	-9.84817	40.57933	1855	2.95[5]	*C~~ib~~. wuellerstorfi*	150 – 250	15
PE304-9	MC	-8.93555	39.61638	370	9.91[5]	*U~~Uvi~~. peregrina~~. spp.~~*	150 – 450	15
						C~~ib~~ibicidoides spp.~~.~~	150 – 450	19
PE304-25	MC	-9.76978	39.91057	482	8.68[5]	*U~~Uvi~~. peregrina~~spp.~~*	250 ~~–~~ – >450	6
PE304-30c	MC	-9.78565	40.22365	1471	4.29[5]	*C~~ib~~ibicidoides spp.~~.~~*	250 – 450	7

BC = box core, MC = multicore

[2, 5] Bottom water temperatures from nearest CTD profiles from Birch et al. (2013): [2] = GLOW Station 2 and [5] = GLOW Station 5.

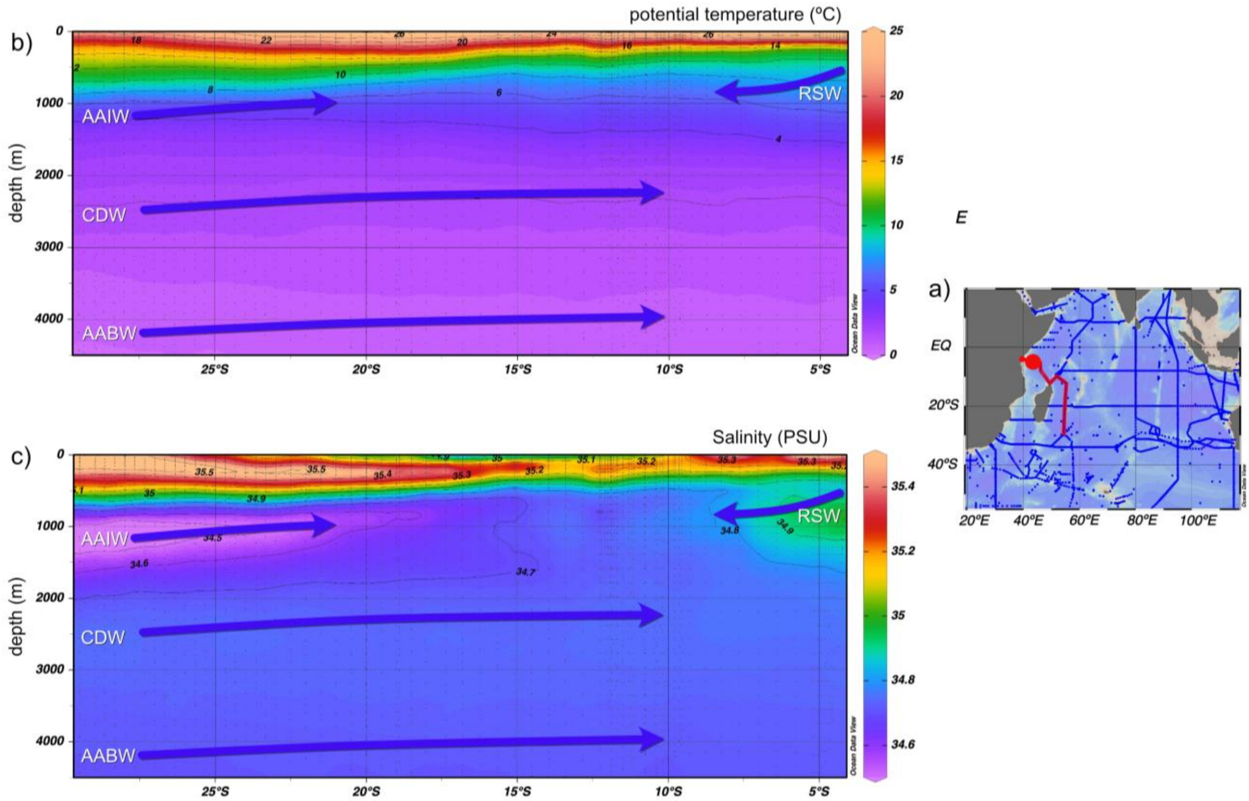

Figure~~.~~ 2.~~.~~ a) Map on the right-hand side shows GLODAPv2_2023 ship tracks and specifically red contours show the transect selected (red dot: nearest available GLDOAPv2_2023 data to core locations in this study). The map has been produced in Ocean Data View. b) and c) North-south cross sections of potential temperature ~~-~~and salinity, respectively, over depths 0-4500 m in the western Indian Ocean from 28˚S to 4˚S. Arrows show flow direction of the main water masses. Temperature and ~~Salinity~~ salinity data from GLODAPv2_2023 (Lauvset et al., 2022; Lauvset et al., 2024). ~~Map produced in Ocean Data View.Panel on the right-hand side show GLODAPv2 ship tracks and specifically red contours show the transect selected (nearest available GLDOAPv2 data to core locations in this study). Map has been produced in Ocean Data View.~~

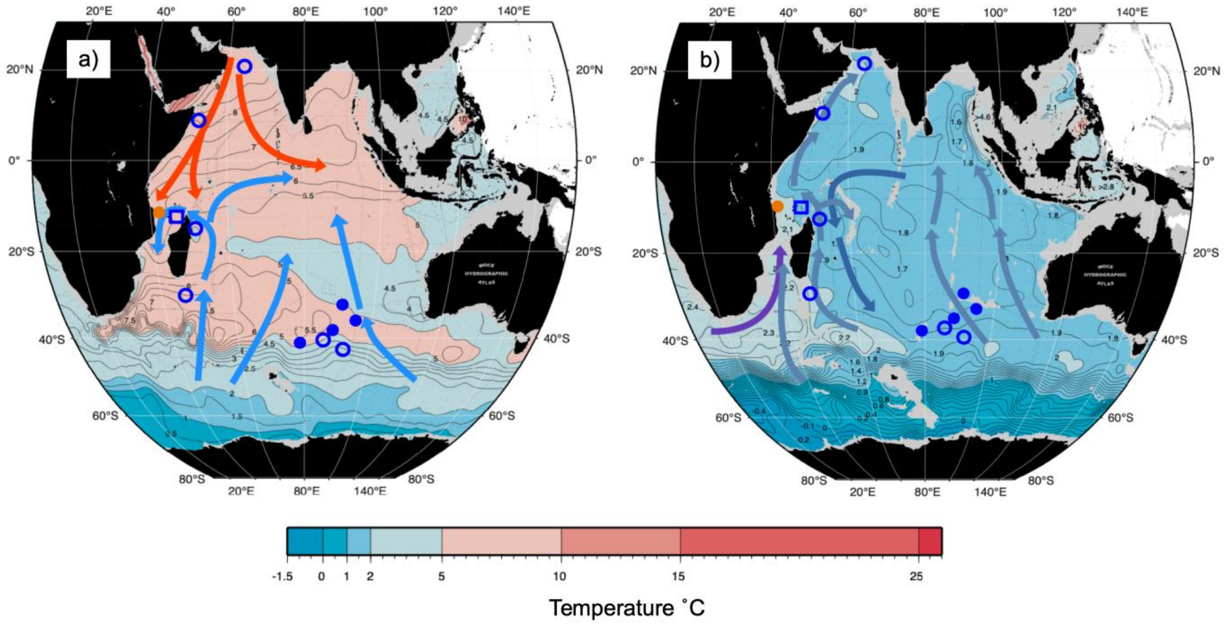

Figure~~.~~ 3.~~.~~ Map of potential temperature adapted from t~~T~~he WOCE Indian Ocean Atlas (Talley et al., 2013) at intermediate and deep-water depths. a) 1000 m with general intermediate water circulation; blue arrow: AAIW and red: RSW b) 2500 m with general deep water circulation; lighter blue arrow: LCDW, darker blue arrow: NIDW/UCDW and purple arrow: NADW.

Approximate location of core-tops from the Indian Ocean; orange circle: this study, open square: nearest CTD transect (Birch et al., 2013), filled circle: Healey et al. (2008) and open circle: Elderfield et al. (2010).

2.2. S~~Core top s~~ample preparation

Mg/Ca can be affected by intra-shell, intra-species, and inter-species variability referred to as 'vital effects' (Bentov and Erez, 2006; de Noijer~~.~~, 2014; and discussions therein). In order to minimize these effects, we have focussed, ~~(~~where possible~~)~~, on analysing multiple whole specimen of three benthic foraminifera species; *U. ~~vigerina~~ peregrina*, *C. ~~ibicidoides~~ wuellerstorfi* and *C. ~~ibicidoides~~ mundulus*. ~~.~~ In most cases these were picked from comparatively small size fraction windows (i.e. 250-355 µm and 250-355 µm). Only in a small number of cases a wider size fraction window was used due to low foraminifera abundances (Table 1).~~-~~ Specimens with no signs of stains, discoloration, fragmentation or post depositional calcification were selected based on previous studies suggesting post depositional effects on Mg/Ca ratios (Lear et al., 2002) (see qualitative observations in Appendix C). Because temperature sensitivity of Mg/Ca in *Cibicidoides spp.* might be species specific (Lea et al., 1999; Gussone et al., 2016), species of *Cibicidoides spp.* were analysed separately except for samples containing less than ~~with abundance <~~5 specimens (Table 1). Sample PE303-18b was split into two to check for intra sample variation (the only sample with sufficient sample size). In order to test the cleaning procedure specimens from the planktic foraminifera species *Globigerinoides~~.~~ ruber* (*G. ruber*) were picked from the 250-355 µm size fraction of samples from core NIOP929 (Saher et al., 2009; core NIOP929 was retrieved from the continental slope off Somalia during the Netherlands Indian Ocean expedition in 1993; van Hinte et al., 1995) because there were insufficient planktic and benthic foraminifera specimens in our off Tanzania core top transect to carry out these tests. The samples ~~have~~ were ~~been~~ wet sieved over a >63µm screen and dried at 40˚C.

All samples were chemically cleaned using water and methanol rinses to remove silicates, a hydrogen peroxide treatment to remove organic matter, and ~~followed by~~ an acid rinse to remove residual treatment chemicals (Barker et al., 2003). The rigour needed to sufficiently clean samples depends on a number of factors including sediment composition and foraminifera morphology, i.e. some species trapping contaminants more than others. ~~Therefore~~Therefore, we have adapted the Mg cleaning methodology by Barker et al., (2003) to find the appropriate level of cleaning required (optimum removal of contaminants while minimising sample loss) for the benthic samples analysed in this study.

In ~~the first~~ experiment 1, 6 sets of specimens of *G~~lobigerinoides~~. ruber* were treated with the chemical cleaning ~~protocol~~ procedure of Barker et al., (2003) ~~was followed~~ except ~~for reducing the time during~~ methanol and MilliQ ~~washes~~ washes were reduced (methanol rinse: 25 seconds repeated twice ~~hrice~~ compared to 1-2 min repeated once – see Table 2 for specifications). ~~following previously analysed samples in the laboratory.~~ The chemicals were prepared following Barker et al., (2003). Traditionally, the procedure involves crushing of foraminifera between two glass plates. Given the small sample volume in our study, we tested individual crushing of foraminifera specimens using a metal pin and glass mortar to open the test chambers. The samples were transferred to Eppendorf tubes with 500 µl MilliQ water and washed with MilliQ followed by washing with methanol, in both steps using an ultrasonic bath. This was followed by a hydrogen peroxide treatment in a hot water bath (30 min at 85˚C) and an acid leach using nitric acid (see protocol in Barker et al., 2003). ~~The samples were transferred to acid-cleaned Eppendorf tubes with 500 µl MilliQ water and washed with MilliQ followed by methanol, both using an ultrasonic bath. This was followed by a hydrogen peroxide treatment in a hot water bath and an acid leach using nitric acid (see protocol in Barker et al., 2003).~~

The results of the first experiment, with some variability, show that average Ca concentrations (normalised to the number of tests) of samples crushed using two glass plates were lower (5.81 ppm, average based on normalised values) than in samples crushed using a metal pin and glass mortar (9.53 ppm, average based on normalised values), see Table A1 and A2 ~~and A2~~ in

Appendix A, suggesting less sample loss in the latter. ~~The~~ The average Mg/Ca ratios of samples crushed using two glass plates and using a metal pin and a glass mortar was broadly similar, i.e. ~~3.43~~4.54 mmol mol^{-1} and ~~3.53~~5.36 mmol mol^{-1}~~,~~ , respectively (please note that we regard sample 1a in Table A2 in Appendix A as an outlier due to the very low Ca concentration). In addition, the range of Mg/Ca values is similar when comparing results using both crushing methods (Table A1 and A2 in Appendix A). Also, the variability between samples is comparable with the range in published data (Sadekov et al., 2008; Rustic et al., 2021)~~respectively (see Table A1 and A2 in Appendix A), suggesting that crushing using a metal pin and glass mortar does not introduce more Mg or Ca bearing contaminants than the technique using two glass plates~~. This suggests that crushing using a metal pin and a glass mortar does not introduce more Mg or Ca bearing contaminants than the technique using two glass plates. Fe and Al concentrations were below the limit of detection in all samples (<0.0070 and <0.0079 ppm) suggesting no silicate contamination. Because the technique using a metal pin and glass mortar entailed less sample loss and there was little difference in Mg/Ca ratios we used this technique for our study.

In experiment 2, as a result of the low Ca concentrations in experiment 1 (0.55 to 7.50 ppm, using either crushing technique, ~~Table 1A and A2 in Appendix A~~ Table 1A and A2 in Appendix A), the chemical cleaning procedure was amended to assess if this was due to calcite dissolution (too rigorous cleaning). In experiment 2, from 8 sets of 20 specimens of *G~~lobigerinoides~~. ruber*, picked from core NIOP929 (Table A1 in Appendix A), four sets were manually crushed using a drop of MilliQ water and a metal pin in a glass mortar. Two of those samples were transferred to a small glass vial and ultrasonicated for 3 seconds. The other two samples were kept intact and transferred to Eppe~~i~~ndorf tubes. The cleaning procedure followed Barker et al. (2003) except for reducing the time ~~during~~ for the methanol step ~~washes~~ (methanol rinse: 20 seconds repeated twice compared to 1-2 min repeated once, see all specifications in Table 2).

Generally, in experiment 2, Ca concentrations are higher than in experiment 1 (range from 7.32 to 30.92 ppm, see ~~Appendix A~~ Table A3 in Appendix A~~2 in Appendix A and Fig. 4~~).~~ ~~ In crushed samples (experiment 2), average Ca concentrations of 15.95~~6~~ ppm (range from 7.92 to 22.54 ppm) are lower than the average in non-crushed samples of 23.~~16~~ 15 ppm (range from 7.32 to 30.92 ppm), suggesting more sample loss from crushing (see ~~Appendix A Table A3~~Table A3 in Appendix A). ~~Because samples that were crushed have a lower~~Based on average Fe/Ca ratios, crushed sample ha~~s~~ve lower Fe/Ca ratios ~~-~~than the uncrushed samples (0.37~~8~~ mmol mol^{-1} compared to 0.57~~61~~ mmol mol^{-1}) suggesting ~~this suggests~~ less silicate contamination in the crushed samples. There is, however, significant uncertainty because the offset is not consistent and one outlier with a substantially higher Fe/Ca ratio (1.56 mmol mol^{-1}) and Mg/Ca ratio (9.41 mmol mol^{-1}) is partly responsible for the higher average (see Fig.~~ure~~ 4a). The strong correlation between Fe/Ca ratios and Mg/Ca ratios in both crushed ($r^2 = 0.99$) and uncrushed ($r^2 = 0.93$) tests suggest insufficient removal of silicate contaminants in both. It is interesting to note that there is only a small difference in average Al/Ca ratios (2.~~91~~ 90 and 3.~~01~~ 02 mmol mol^{-1}) with no linear ~~correlation~~ correlation ~~with~~ to Mg/Ca ratios (Fig.~~ure~~ 4b) which suggest only ~~no~~ a small difference in ~~difference in~~ silicate contamination. The strong correlation between Mn/Ca ratios and Mg/Ca ratios in ~~both~~ crushed samples ($r^2 = 0.95$) suggests insufficient removal of Mn-oxide coatings. Similarly, Mn/Ca ratios and Mg/Ca ratios in ~~and~~ uncrushed ($r^2 = 0.95$) tests also ~~-~~suggest insufficient removal of Mn-oxide coatings in both, although this correlation depends on a potential outlier. ~~This~~ These findings support~~s~~ the notion that, regarding Mn-oxide coatings, the rigour of the chemical cleaning is significantly more important than mechanical crushing. From the inconclusive results and because of time constraints, we decided to crush shells prior to chemical cleaning in the subsequent ~~Overall, the outcomes from experiment 2 suggest that crushing of foraminifera ensures better cleaning results. Due to time constraints we decided to crush shells prior to chemical cleaning in the subsequent~~ ~~E~~experiment 3 following previous benthic core-top studies (Elmore et al., 2015; Elderfield et al., 2010; Barker et al., 2003).

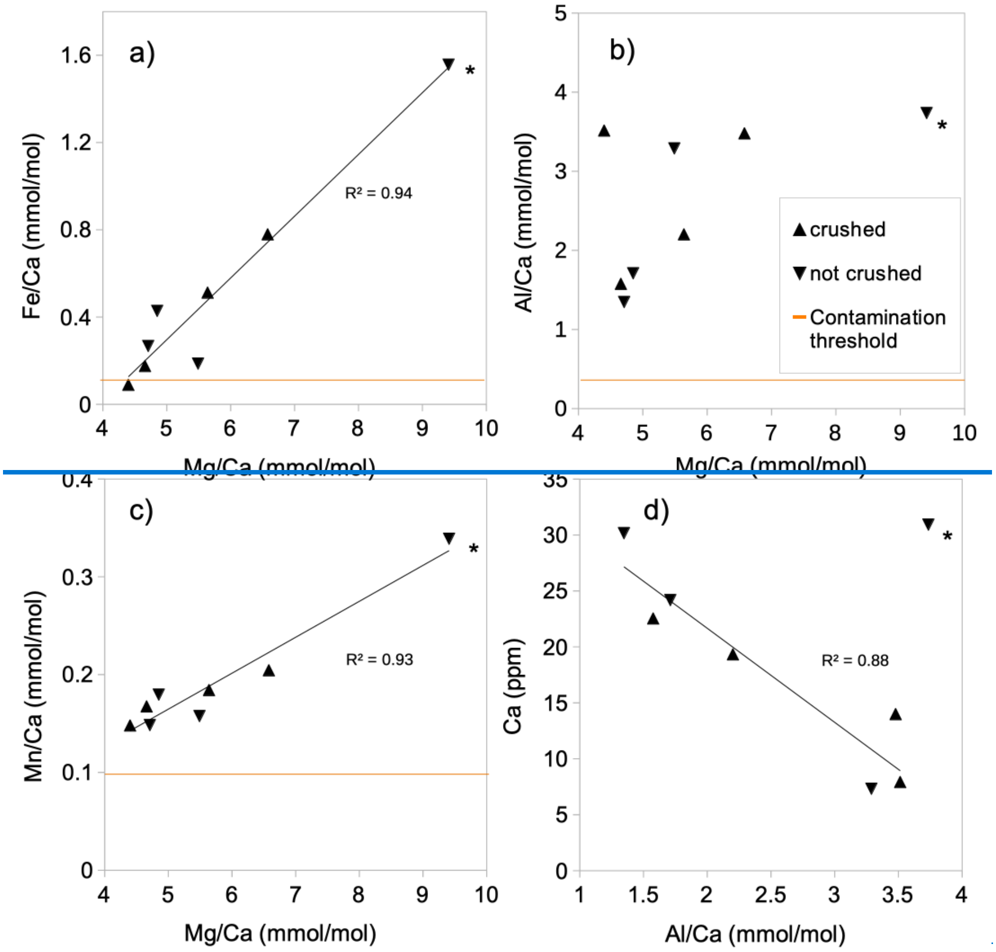
a)
Fe/Ca (mmol/mol)
Mg/Ca (mmol/mol)
R² = 0.94
b)
Al/Ca (mmol/mol)
Mg/Ca (mmol/mol)
crushed
not crushed
Contamination threshold
c)
Mn/Ca (mmol/mol)
Mg/Ca (mmol/mol)
R² = 0.93
d)
Ca (ppm)
Al/Ca (mmol/mol)
R² = 0.88

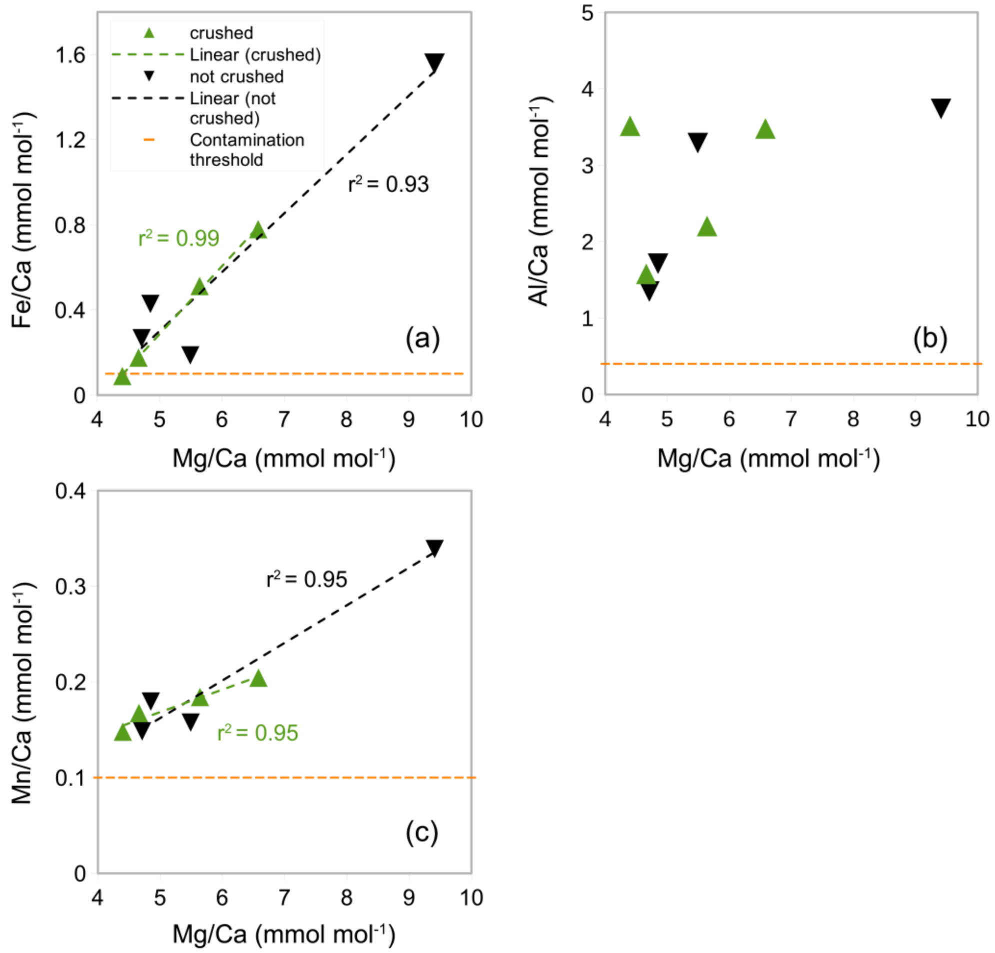

Figure~~.~~ 4. Mg/Ca ratios in *G. ruber* in NIOP929 (Saher et al., 2009) using the procedure of Experiment 2. **a.** Correlation between Fe/Ca ratios and Mg/Ca ratios in crushed and uncrushed samples~~. See comments in text regarding sample with high Fe/Ca and Mg/Ca ratios. With this sample being include, R^2 is 0.94. Without this sample R^2 is 0.72~~. See comments in the text regarding the sample with high Fe/Ca and Mg/Ca ratios. **b.** no correlation between Al/Ca ratios and Mg/Ca ratios. **c.** Correlation between Mn/Ca ratios and Mg/Ca ratios. Orange horizontal lines: Fe/Ca, Al/Ca and Mn/Ca contamination thresholds (0.1, 0.4 and 0.1 mmol mol^{-1} respectively). ~~(R^2=0.93 with outlier and R^2=0.65 without **d.** Correlation between Ca concentrations and Al/Ca ratios, R^2=0.88 when outlier * is excluded.~~

In Experiment 3, Eppendorf tubes were acid-cleaned and ~~the cleaning procedure followed Barker et al. (2003) with an additional 20 seconds~~ methanol rinses ~~total time of methanol wash added based~~increased based on the contamination post-cleaning identified in Experiment 2 (35 seconds repeated thrice which closely follow Barker et al.'s (2003) total time of 1-2 min repeated twice - see Table 2 for specifications). S~~In the procedure, s~~pecimens of *G.~~Globigerinoides~~ ruber* (6 sets with a varying amount of 10 - 50 specimen~~of x25 specimens~~) picked from core NIOP929, *Uvigerina~~vig erina.~~ spp.* (10 specimens) from core PE303-17a, and *Cibicidoides spp.* (2 sets of ~~x~~5 specimens) from cores PE303-17Aa and PE303-13b (Table A1 in Appendix A~~Appendix A Table A1~~) were used.

In contrast to Experiment 2, there is no correlation between Mg/Ca ratios and Al/Ca (Fig.~~ure~~ 5a) and only a weak correlation between Mg/Ca ratios and Mn/Ca (Fig.~~ures~~ 5c) and most samples have Fe concentrations below the limit of detection (<0.0058 ppm). This suggests no or minimal silicate contamination and Mn-oxide coatings (Barker et al., 2003; Elderfield et al., 2010). The average Al/Ca ratios in samples containing Al concentrations above the limit of detection (6 out of 9) is significantly above the threshold for contamination (>0.4 mmol mol^{-1}), 2.27 mmol mol^{-1} (Fig.~~ure~~ 5a, Table A3 in ~~Table A3 in~~ Appendix A ~~Table A3~~) but because there is no correlation with Mg/Ca ratios this could be due to issues with precision of measurements as reported by Elderfield et al., (2010) or due to contamination from contaminants other than silicate. The Al/Ca ratios showed a negative exponential correlation with Ca concentrations (Fig.~~ure~~ 5b) where high Al/Ca ratios correlated with low Ca concentration. This could suggest that there is a threshold for a minimum Ca concentration for contaminants to accurately be determined. According to the exponential relationship of Al/Ca ratios and Ca concentrations in Fig. 5b, it is suggested that there is a threshold for total Ca concentration between 15 and 25 ppm. The average Mn/Ca ratio was 0.16 mmol mol^{-1} (Fig.~~ure~~ 5c) which is slightly above the contamination threshold >0.1 mmol mol^{-1}, but below the contamination threshold of 0.2 mmol mol^{-1} proposed by Hasenfratz et al. (2017). This suggest~~ing~~ that Mn-oxide coatings have an insignificant effect on Mg/Ca ratios.

Based on the results from Experiment 3, indicating no or minor silicate contamination and Mn-oxide coatings, the cleaning methodology of core-tops followed the methodology used in Experiment 3, i.e. Barker et al. (2003)~~-~~. A summary of the differences in cleaning methodology used in this study is found in Table 2.

Table 2. Specifications of chemical cleaning procedures used in Experiments 1-3 and core-top analysis

Experiment	Species type	Methodology	Specifications	Preparation
1	*Planktic only*	Barker et al., 2003 with adjustments	MilliQ rinse: three 25 s rinses[U] Methanol rinse: two 25 s rinses[U] Hydrogen peroxide 85˚C 30 min Weak acid leach (nitric acid)	Crushing/No crushing
2	*Planktic only*	Barker et al., 2003 with adjustments	MilliQ rinse: three 20 s rinses Methanol rinse: two 20 s rinses Hydrogen peroxide 30 min at 85˚C Weak acid leach (nitric acid)	Crushing
3	*Planktic and Benthic*	Barker et al., 2003 with minor adjustments	Acid cleaned Eppendorf tubes MilliQ rinse: four 25 s Methanol rinse: four 35 s rinses Hydrogen peroxide 30 min at 95˚C Weak acid leach (nitric acid)	Crushing
Core-tops	*Planktic and Benthic*	Barker et al., 2003 with minor adjustments	Same as Experiment 3	Crushing

[U] seconds refers to time in ultrasonic bath at 50% power.

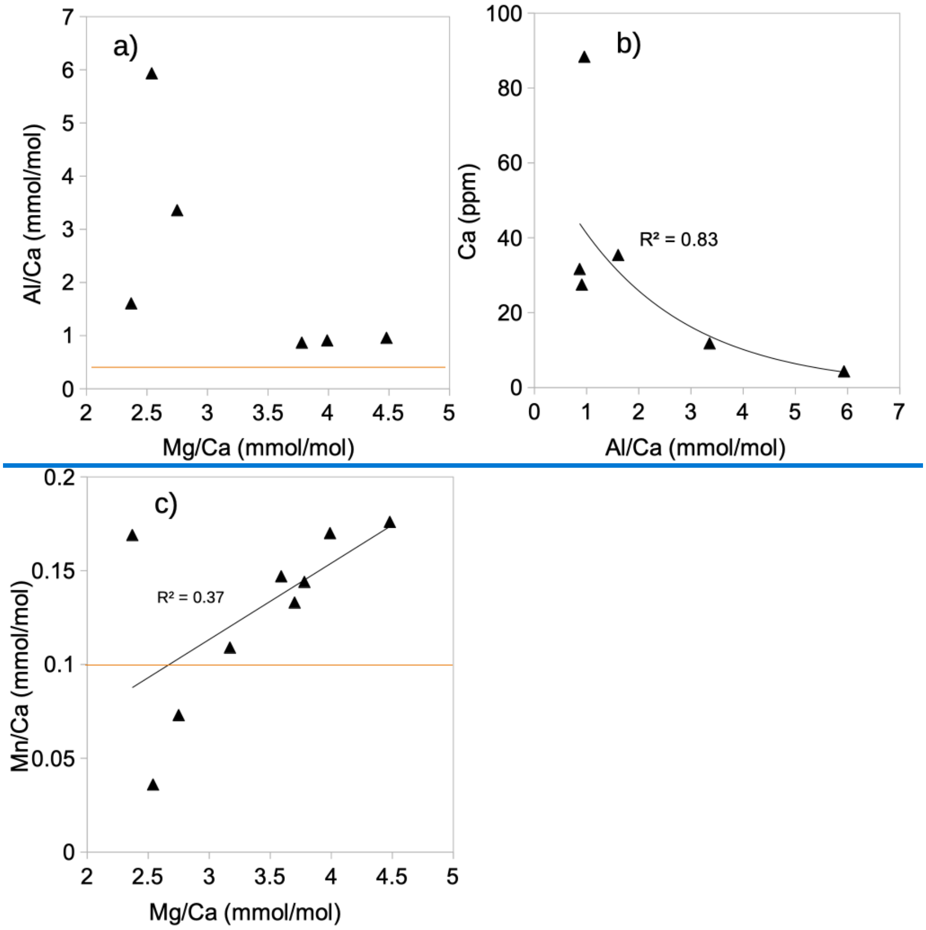
a)
Al/Ca (mmol/mol)
Mg/Ca (mmol/mol)
b)
Ca (ppm)
R² = 0.83
Al/Ca (mmol/mol)
c)
Mn/Ca (mmol/mol)
R² = 0.37
Mg/Ca (mmol/mol)

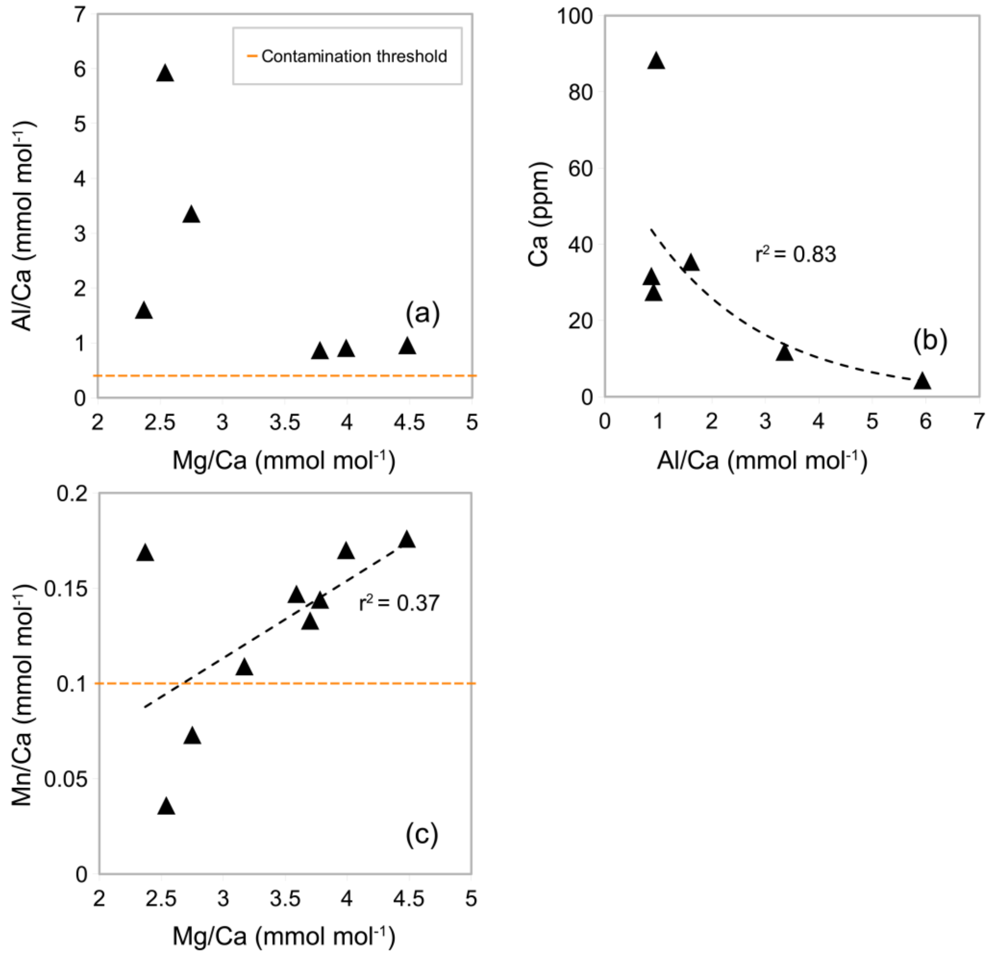

Figure ~~.~~5~~.~~: Correlation between **a.** Al/Ca ratios and Mg/Ca ratios, **b.** Ca concentration and Al/Ca ratios, **c.** Mn/Ca ratios and Mg/Ca ratios of samples of *G. ruber* from core NIOP929 following procedure in Experiment 3. Orange horizontal lines: Al/Ca and Mn/Ca contamination thresholds (0.4 and 0.1 mmol/mol respectively).

2.3. Mg/Ca analysis in ICP-OES

Supernatants (300 µl) of the dissolved samples were transferred to acid-cleaned polypropylene tubes and diluted to 1.8 ml with dilute HNO_3. Samples were analysed in an ICP-OES Varian Vista Pro at the Grant Institute at The University of Edinburgh.

Emission intensity was normalised to concentrations using a standard calibration curve based on measurements of high purity standards (~~element calibrations and concentration of standards in Figure 1 and Table B1 in Appendix B~~ Fig. B1 and Table B1 in Appendix B). Analytical lines (Mg) 285 and (Ca) 315 are used as these are reported to minimise matrix effect (De Vielliers et al., 2002). Instrumental precision was ± 1% based on 6 replicate measurements of the ECRM 752-1 carbonate standard. The limit of detection was calculated by 3 multiples of the standard deviation. The calibration curves of the standards have an R~~r~~^{2} > 0.99 (Table B1 in Appendix B~~Appendix B Fig.ure B1~~). To overcome matrix effects associated with Ca analysis, a calibration was produced using standard solutions of increasing Mg/Ca ratios (~~Appendix B~~ Table B1 in Appendix B) as described by De Vielliers et al. (2002). In addition, the ECRM was diluted to a concentration of 40 ppm Ca (similar to the concentrations of the samples studied) which also assumes a similar matrix effect. Two procedural blanks and two samples of the ECRM-752-1 carbonate standard with a Mg/Ca ratio of 3.762 mmol mol^{-1} were included in every run. In addition to Mg/Ca, Fe/Ca, Al/Ca and Mn/Ca were calculated to monitor silicate contamination and Mn-oxide coatings (Barker et al., 2003).

Following Barker et al. (2003) and Elderfield et al. (2010) contamination thresholds of Fe/Ca, Al/Ca and Mn/Ca ratios used were 0.1, 0.4 and 0.1 mmol mol^{-1}, respectively. Linear regression was plotted between Fe/Ca, Al/Ca, Mn/Ca ratios and Mg/Ca ratios and the ~~r^2~~ r^2 value was used to assess if there was a significant correlation. Procedural blanks were used to correct Mg, Ca, Fe, Al and Mn concentrations for any introduced contaminants. Mg/Ca ratios were calculated using Ca315 and Mg285 concentrations in ppm and ppb, corrected by blanks and converted to mmol mol^{-1} by:

$$\text{Mg/Ca} = \frac{(Mg285\,(ppb) - Mg285_{blank})/M_{Mg}}{(Ca315(ppm) - Ca315_{blank})/M_{Ca}}$$

where M_{Mg} and M_{Ca} refers to the atomic masses of Mg (24.305 g mol^{-1}) and Ca (40.08 g mol^{-1}). This ~~was~~ approach was also used for Fe/Ca, Al/Ca, Mn/Ca using their respective atomic masses (M_{Fe}, M_{Al} and M_{Mn}).

2.4. Mg/Ca – BWT calibration

A linear regression was applied to assess the correlation between the Mg/Ca ratios measured in *C.* ~~*ibicidoides*~~ *wuellerstorfi*, *C.* ~~*ibicidoides*~~ *mundulus*, *U.* ~~*vigerina*~~ *peregrina* and *Cibicidoides* ~~-~~*spp*. and modern bottom water temperatures from the nearest hydrographic temperature profile (see Table 1). The slope of Mg/Ca ratios over BWT ~~were~~ was compared with previous studies from the Atlantic, Pacific and Indian Ocean.

3. RESULTS

3.1. ~~Core-top Mg/Ca~~Elemental ratios of~~in~~ *Cibicidoides spp.* in core tops

In samples (Table 1) containing *C.* ~~*ibicidoides*~~ *wuellerstorfi* and *C.* ~~*ibicidoides*~~ *mundulus* the Ca concentrations range from 4.00 to 68.72 ppm (see Table ~~2~~3). Mg/Ca ratios range from 1.19 to 6.04 ± 0.03 mmol mol^{-1} in *Cibicidoides spp.* (12 samples, Table 3), and 3.17 to 4.18 ± 0.05 mmol mol^{-1} in *G. ruber* (6 samples, ~~Appendix A~~ Table A4 in Appendix A). The Fe/Ca ratios range from 0.13 to 0.35 mmol mol^{-1} in *C.* ~~*ibicidoides*~~ *wuellerstorfi*, from 0.98 to 1.10 mmol mol^{-1} in *C.* ~~*ibicidoides*~~ *mundulus* and 0.08 to 2.45 mmol mol^{-1} in *Cibicidoides spp*. All six samples of *G. ruber* (analysed in the same run, from core NIOP929) have Fe concentrations below the limit of detection (<0.0034 ppm, ~~see Table A3 in~~ Table A4 in Appendix A~~Appendix A Table A4~~). The Al/Ca ratios range from 0.28 to 0.57 mmol mol^{-1} in *C.* ~~*Cibicidoides*~~ *wuellerstorfi*, from 0.24 to 2.66 mmol mol^{-1} in *C.* ~~*ibicidoides*~~ *mundulus*, from 0.21 to 0.36 mmol mol^{-1} in *Cibicidoides spp*. (Table ~~2~~3) and from 0.25 ~~and~~ to 0.37 mmol mol^{-1} in *G. ruber* (~~Table A3 in~~ Table A4 in Appendix A~~Appendix A Table A4~~). The Mn/Ca ratios range from 0.01 to 0.20 mmol mol^{-1} in *Cibicidoides spp.* samples (Table ~~2~~3) and from 0.13 to 0.19 mmol mol^{-1} in the planktic samples (~~Table A3 in~~ Table A4 in Appendix A~~Appendix A Table A4~~). There is no obvious correlation between the Fe/Ca, Al/Ca and Mn/Ca with Mg/Ca ratios for any of the *Cibicidoides* species, except for *C.* ~~*ibicidoides*~~ *mundulus* (Fig.~~ure~~ 6a~~-a, b,~~ c). In this figure, although mostly driven by one possible outlier, a correlation of Al/Ca with Mg/Ca might be indicated. Regarding contamination thresholds of 0.1~~-~~, 0.4 and 0.1 mmol mol^{-1} for~~–~~ the Fe/Ca, Al/Ca and Mn/Ca ratios, respectively, all *Cibicidoides spp.* samples are below the threshold for Al/Ca and Mn/Ca ratios. In relation to the Fe/Ca ratio, one sample was below, one sample just above and three samples well above the contamination threshold (Table ~~2~~3).

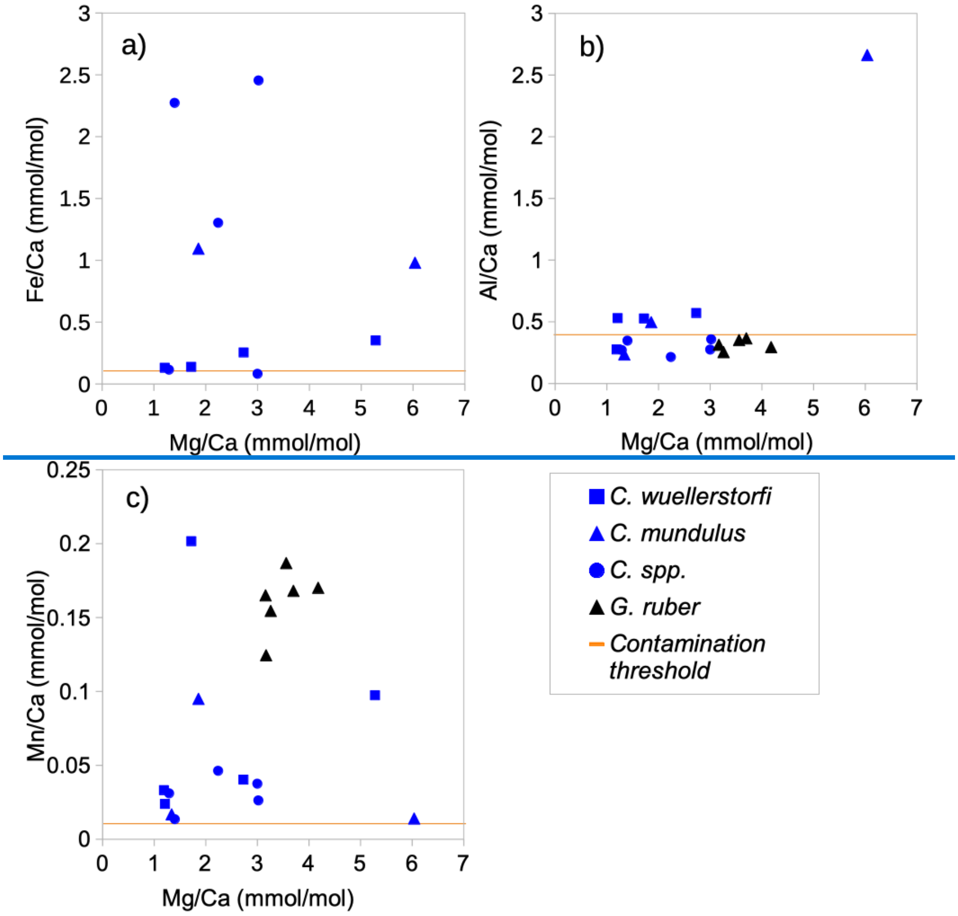

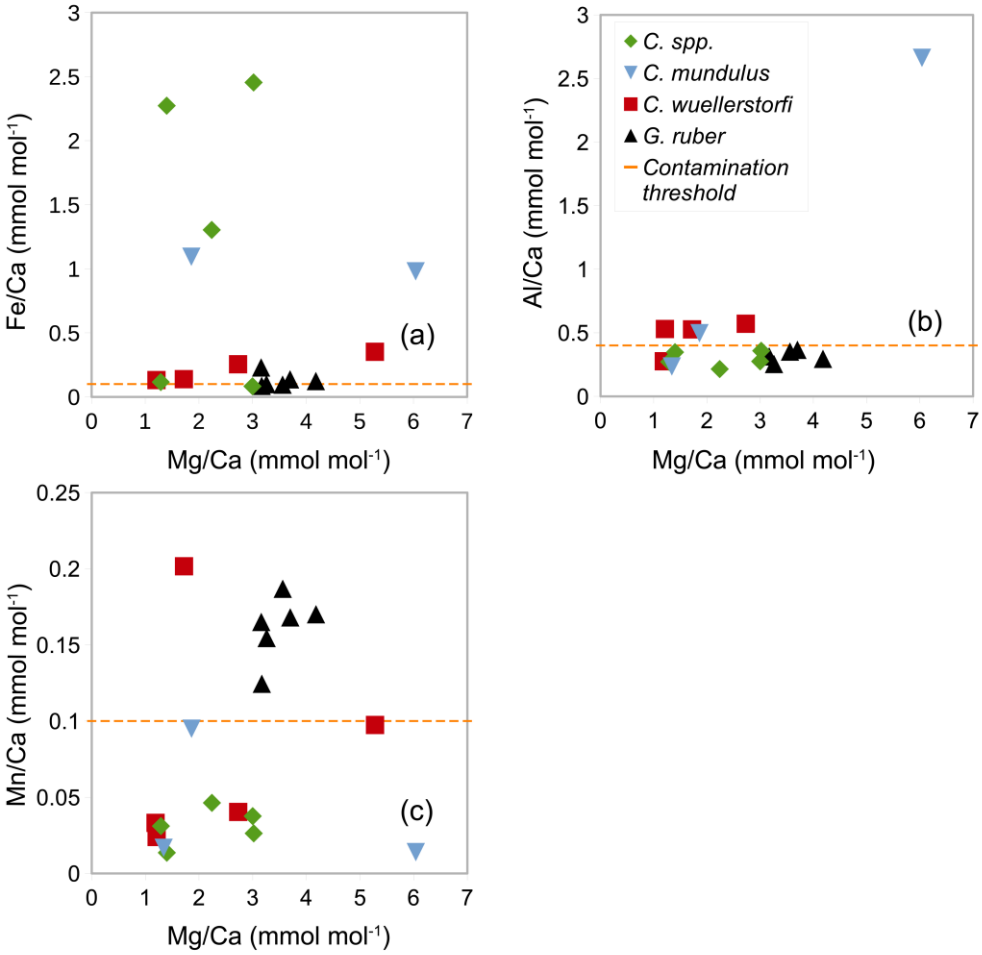

Figure~~.~~ 6. Correlation between **a.** Fe/Ca ratios, **b.** Al/Ca ratios, **c.** Mn/Ca ratios and Mg/Ca ratios in *Cibicidoides spp.* including

C. wuellerstorfi and *C. mundulus* and *G. ruber* (control group). ~~). **d.** The correlation between total Ca concentration and contamination (Fe/Ca ratios).~~ The orange horizontal lines show the respective contamination ~~show~~ thresholds -at ~~at~~ 0.1, 0.4 and 0.1 mmol mol^{-1} ~~as an indication of contamination~~for Fe/Ca, Al/Ca and Mn/Ca following Barker et al. (2003).

Table~~.~~ 3~~2~~. Mg/Ca ratios, contamination indicators (Fe/Ca, Al/Ca and Mn/Ca ratios) and Ca measured in *C. wuellerstorfi*, *Cibicidoides~~.~~ spp.*, *C. mundulus* and *U. peregrina* from Tanzania core-top samples.

Core	Species	Mg/Ca	Fe/Ca	Al/Ca	Mn/Ca	Ca	Note
PE303-4c	*C. wuellerstorfi*	1.19	<LOD	0.28	0.03	16.05	
PE303-6a	*C. wuellerstorfi*	1.72	0.14*	0.53*	0.20*	35.09	
PE303-3	*C. wuellerstorfi*	1.21	0.13*	0.53*	0.02	68.73	
PE303-22	*C. wuellerstorfi*	5.28	0.35*	<LOD	0.10	3.99	?
PE303-18b	*C. wuellerstorfi*	2.73	0.25*	0.57*	0.04	14.43	?
PE303-6a	*C. mundulus*	1.86	1.09*	0.49*	0.10	20.56	e
PE303-3	*C. mundulus*	1.34	<LOD	0.23	0.02	15.84	
PE303-18b	*C. mundulus*	6.04**	0.98*	2.66*	0.01	55.91	e
PE303-3	*Cibicidoides~~.~~ spp.*	1.40	2.27*	0.34	0.01	17.27	e
PE303-14a	*Cibicidoides~~.~~ spp.*	1.29	0.12*	0.27	0.03	75.62	
PE304-9	*Cibicidoides~~.~~ spp.*	3.02	2.45*	0.35	0.03	30.96	e
PE304-30c	*Cibicidoides~~.~~ spp.*	2.24	1.30*	0.21	0.05	22.22	e
PE303-50	*Cibicidoides~~.~~ spp.*	3.00	0.08	0.27	0.04	28.53	
PE303-6a	*U. peregrina*	1.17	0.02	0.91*	0.05	18.54	n
PE303-14a	*U. peregrina*	1.10	0.15*	0.68*	0.009	17.61	e
PE303-6a	*U. peregrina*	2.17	0.67*	1.09*	0.07	16.28	e
PE303-4c	*U. peregrina*	1.58	0.07	0.71*	0.03	20.35	
PE303-17a	*U. peregrina*	2.99	1.66*	2.34*	0.06	41.28	e
PE304-9	*U. peregrina*	1.82	0.43*	1.42*	0.009	68.17	e
PE303-18b (1)	*U. peregrina*	2.76	2.02*	4.02*	0.02	79.35	e
PE303-18b (2)	*U. peregrina*	2.52	1.55*	3.90*	0.02	74.32	e
PE304-25	*U. peregrina*	2.69	2.04*	3.61*	0.06	65.80	e

*above contamination threshold 0.1, 0.4 and 0.1 mmol mol^{-1} for Fe/Ca, Al/Ca and Mn/Ca (Elderfield et al., 2010)

**clear outlier based on typical Mg/Ca range reported in previous studies

e = excluded due to high contamination, ? = ambiguous assessment of contamination

<LOD = below limit of detection

n = not excluded based on Elderfield et al., 2006 suggesting not to exclude samples based on Al/Ca above 0.4 mmol mol^{-1} alone, both Mn/Ca and Fe/Ca <0.1 mmol mol^{-1}

3.2. Elemental ratios of ~~Core-top Mg/Ca ratios in~~ *Uvigerina peregrina* in core tops

In the core-top samples (Table 1) the Ca concentration in *U. ~~vigerina~~ peregrina*, range from 16.28 to ~~74~~79.~~32~~35 ppm (Table 3~~2~~). The Mg/Ca ratios vary between 1.10 and 2.99 mmol mol^{-1} ± 0.02 mmol mol^{-1} in *U. ~~vigerina~~ peregrina* (9 samples), and between 4.77 and 5.22 ± 0.05 mmol mol^{-1} in *G. ruber* (3 samples analysed in the same run from core NIOP929; Fig.~~ure~~ 7 and Table A4 in Appendix A~~Table 3~~~~2~~). The Fe/Ca ratios range from 0.02 to 2.04 mmol mol^{-1} in *U. ~~vigerina~~ peregrina* and from 0.24 to 0.38 mmol mol^{-1} in *G. ruber*. The Al/Ca ratios are between 0.68 and 4.02 mmol mol^{-1} in *U. ~~vigerina~~ peregrina* and range from 0.92 to 1.31 mmol mol^{-1} in *G. ruber*. The Mn/Ca ratios vary between 0.01 and 0.~~08~~07 mmol mol^{-1} in *U. ~~vigerina~~ peregrina* and 0.11 and 0.14 mol mol^{-1} in *G. ruber*. There is a strong positive correlation (~~r^2~~ r^2 = 0.87) between the Fe/Ca ratios and the Mg/Ca ratios (Fig.~~ure~~ 7a~~.~~) and a positive correlation (~~r^2~~ r^2 = 0.66) between the Al/Ca ratios and the Mg/Ca ratios (Fig.~~ure~~ 7b~~.~~). There is no correlation between the Mn/Ca ratios and the Mg/Ca ratios (Fig.~~ure~~ 7c). Regarding contamination, all *U. ~~vigerina~~ peregrina* samples are below the threshold for Mn/Ca ratios. All samples are above the threshold for Al/Ca ratios, some rather narrowly so. Two samples were below the threshold for Fe/Ca, one narrowly above and the remaining 6 samples partially well above the limit (Table 3~~2~~).

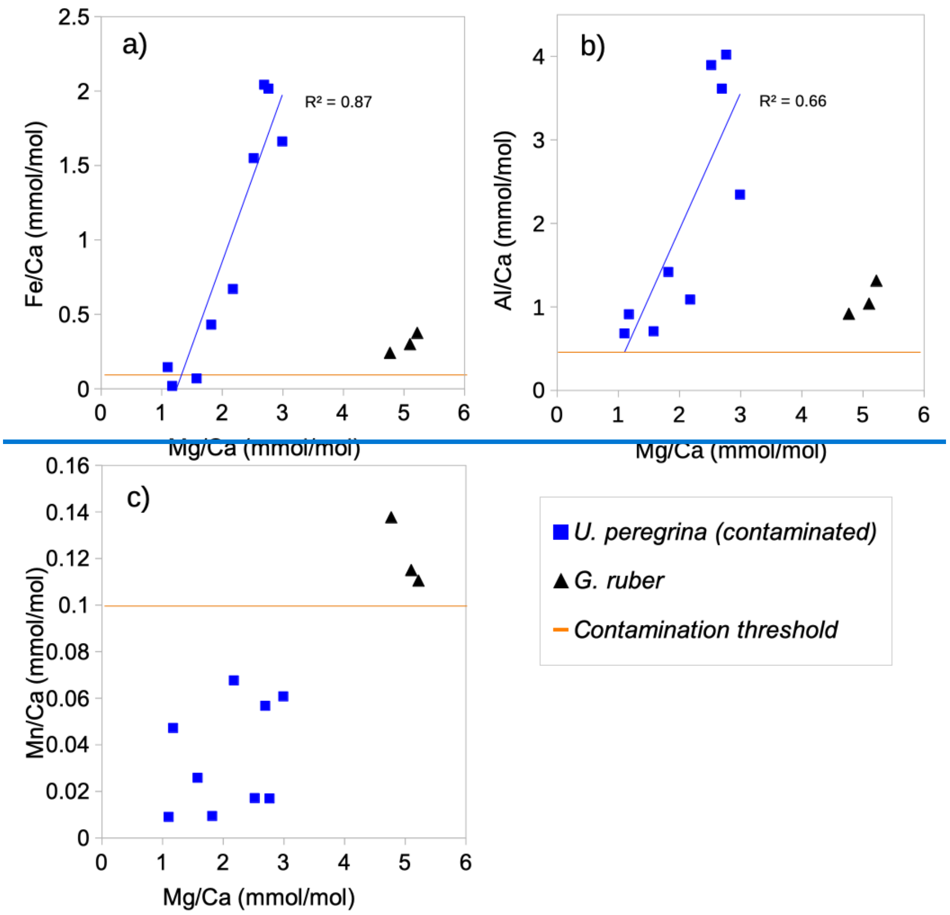

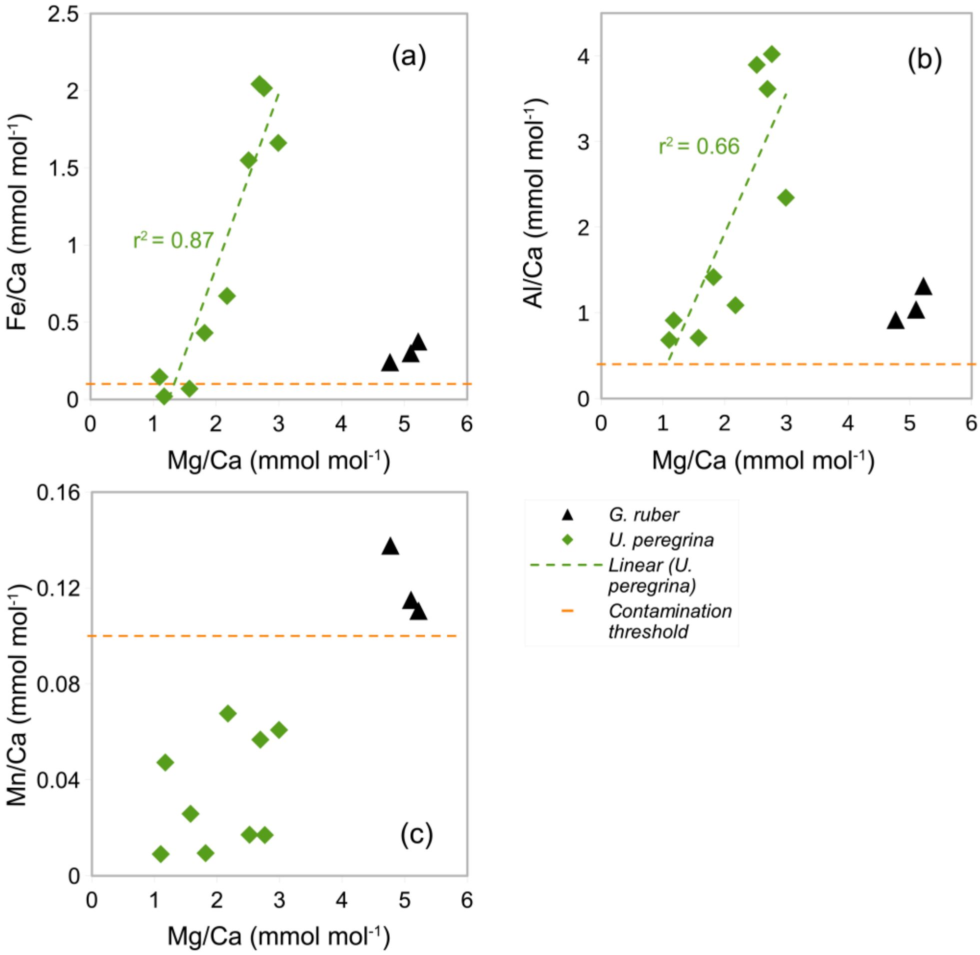

Figure~~.~~ **7**.~~:~~ The correlation between the Mg/Ca ratios and **a.** Fe/Ca ratios, **b.** Al/Ca ratios and **c.** Mn/Ca ratios in blue: ~~*Uvigerina*~~ *U.* *peregrina* and black: *G. ruber* (control group). Horizontal lines show Fe/Ca, Al/Ca and Mn/Ca contamination thresholds (0.1, 0.4 and 0.1 mmol mol^{-1}). Values below the limit of detection are not plotted. Trendline in a. and b. with ~~R^2~~ r^2 show linear correlation of *U.* ~~*vigerina*~~ *peregrina*.

3.3. Correlation between contamination and core-top depth

Fig.~~ure~~ 8a-b shows Fe/Ca and Al/Ca ratios from *U.* ~~*vigerina*~~ *peregrina* and *Cibicidoides spp.* versus the retrieval depth of the samples. There is no correlation between Fe/Ca- or the Al/Ca ratios and depth for *Cibicidoides*~~.~~ *spp.* while *U.* ~~*vigerina*~~ *peregrina* displays such correlations with ~~r^2~~ r^2 values of 0.58 and 0.65, respectively. In water depth ~~<~~>~~Below~~ 2500 m, ~~,~~ *U.* ~~*vigerina*~~ *peregrina* (~~five~~ four samples) shows significantly smaller average Fe/Ca and Al/Ca ratios (0.23 and 0.85 mmol mol^{-1}) compared to samples from <1500 m (~~four~~ five samples) (1.54 and 3.06 mmol mol^{-1}).

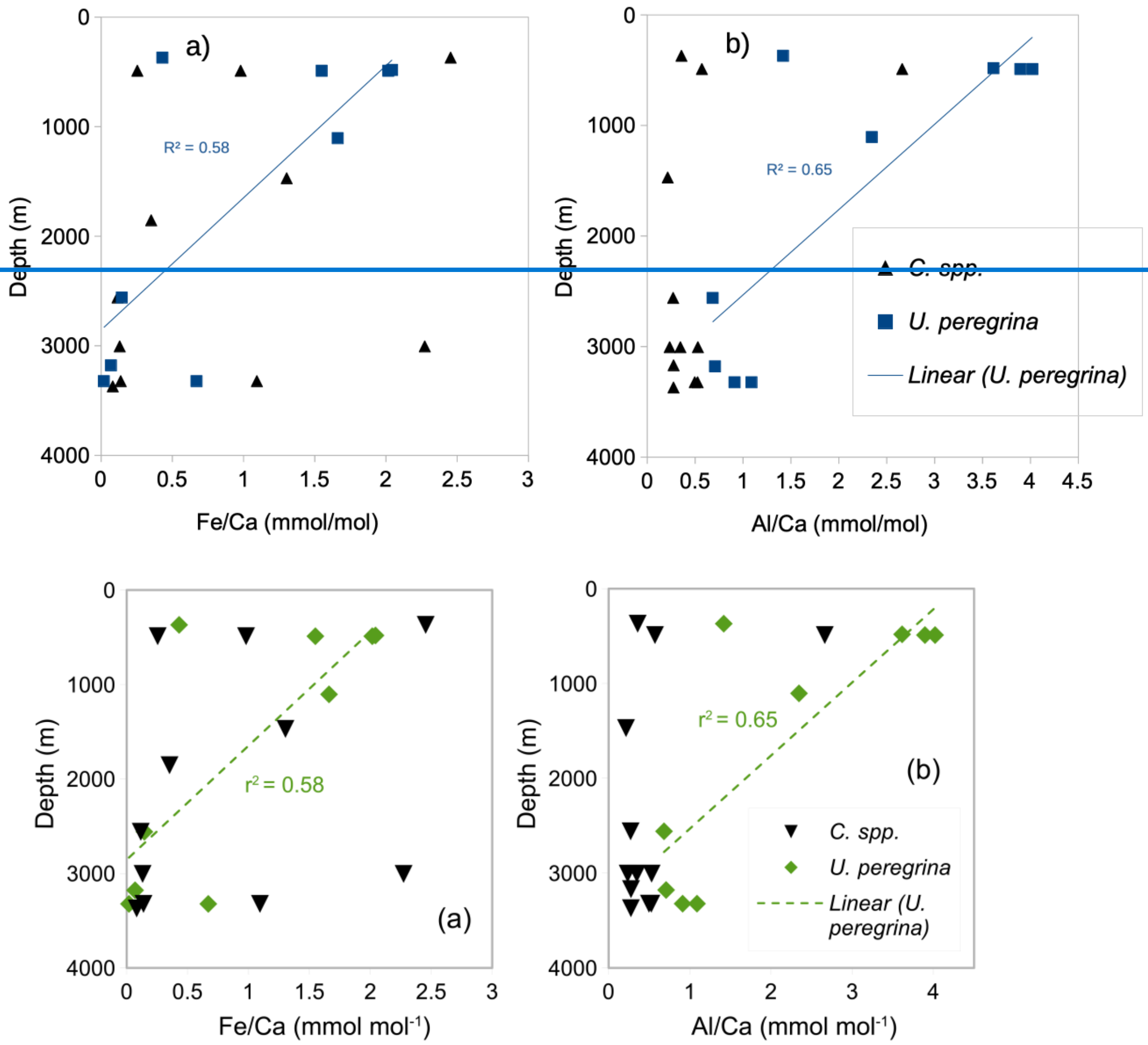

Figure~~.~~ **8**.~~:~~ Correlation between water depth of sediment surface samples and contamination (**a.** Fe/Ca and **b.** Al/Ca) in *Uvigerina peregrina* and *Cibicidoides spp* ~~*Cibicidoides species*~~.

3.4. Mg/Ca – BWT calibration

Principally we used the thresholds of 0.1, 0.4 and 0.1 mmol mol^{-1} of Fe/Ca, Al/Ca and Mn/Ca ratios following Elderfield et al. (2010) and Barker et al. (2003) as well as correlations between Fe/Ca, Al/Ca and Mn/Ca ratios with Mg/Ca ratios following Barker et al. (2003) to assess silicate and/or Mn-oxide contamination. All but two samples of *U.* ~~*vigerina*~~ *peregrina* (Table 3~~2~~) were excluded due to high Fe/Ca ratios (>0.1 mmol mol^{-1}) and a strong correlation with Mg/Ca (Fig.~~ure~~ 7a). Some of the Mg/Ca ratios of *Cibicidoides spp.* were included even though Fe/Ca ratios were >0.1 mmol mol^{-1} ~~samples with Fe/Ca ratios >0.1 and <0.3 mmol mol^{-1} were included which showed no correlation between Fe/Ca ratios~~ since they show no correlation between Mg/Ca ratios and Fe/Ca ratios ~~and Mg/Ca ratios~~ (Table ~~-~~3~~2~~, Fig.~~figure~~ 6). The Mg/Ca ratios not included in core-top calibration are in Table 3~~2~~ (annotated 'e').~~.~~

The Mg/Ca ratios of *Cibicidoides* ~~*ibicidoides*~~ *spp.*~~.~~, *C. mundulus* and *C.* ~~*ibicidoides*~~ *wuellerstorfi* (Table 3~~2~~) were plotted versus BWT (temperature profiles from positions close to our core-top transect from Birch et al., 2013; Fig.~~figure~~ 9). For *Cibicidoides* ~~*C.ibicidoides.*~~ *spp.*, *U.* ~~*vigerina*~~ *peregrina* and *C.* ~~*ibicidoides*~~ *mundulus* discerning robust relationships between the Mg/Ca relationships and ~~BTW~~ BWT is not straightforward. Based on the no-correlation argument above, and ignoring contamination thresholds, tentative relationships are indicated for *Cibicidoides* ~~*Cibicidoides.*~~ *spp.* and *C.* ~~*ibicidoides*~~ *mundulus*. These are, however, partially based on samples with signs of contamination being reflected in the Fe/Ca and/or the Al/Ca ratios.

Removing those samples entails an insufficient amount of data remaining to establish a relationship (~~see~~ Fig.~~figure~~ 9). For *C.* ~~*ibicidoides*~~ *wuellerstorfi* there is little indication of strong contamination. Only some Al/Ca ratios are slightly above the contamination threshold. Establishing a straightforward relationship of Mg/Ca with B~~T~~WT is hampered by one sample with unusually high Mg/Ca values. We regard this sample as an outlier for an unknown reason. Fig.~~gure~~ 9 shows the resulting relationship for *C.* ~~*ibicidoides*~~ *wuellerstorfi* (n=4, see formula below) alongside the remaining samples for the other species. In Fig. 9 the linear correlation for *C.* ~~*ibicidoides*~~ *wuellerstorfi* is:

$$\mathrm{Mg/Ca} = 0.19 \pm 0.02 * \mathrm{BWT} + 1.07 \pm 0.03,\ \cancel{r}r^2 = 0.87$$

The standard error of the regression is 1.55˚C, which is broadly in line with published data (Lear et al., 2002; Sadekov et al., 2008).

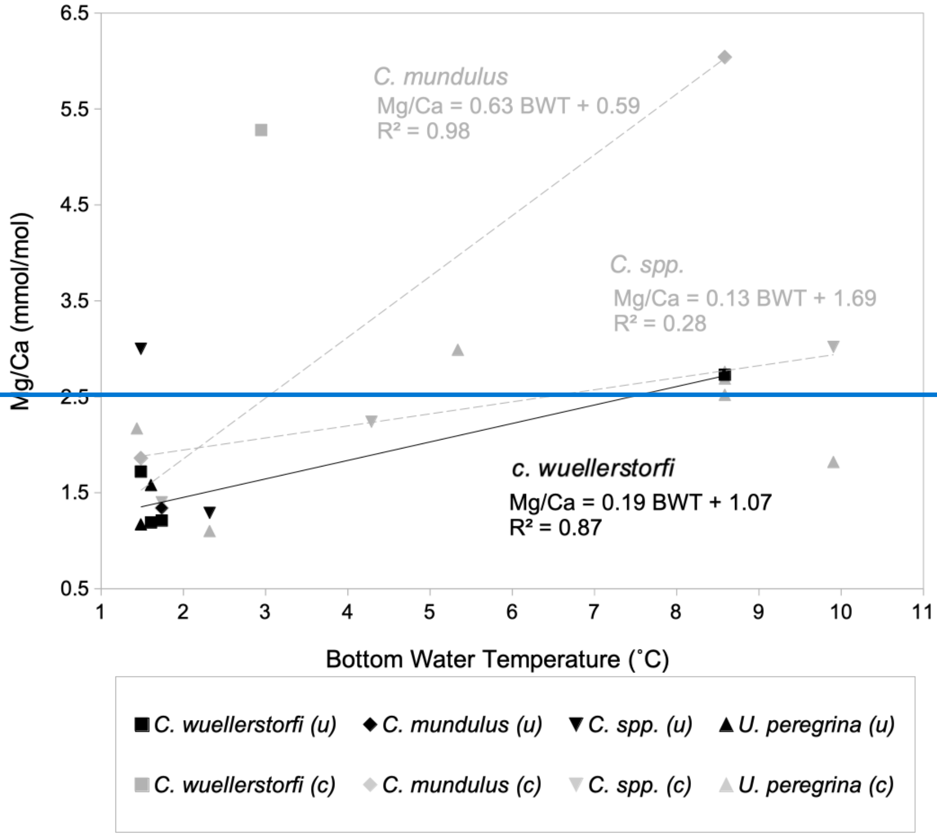

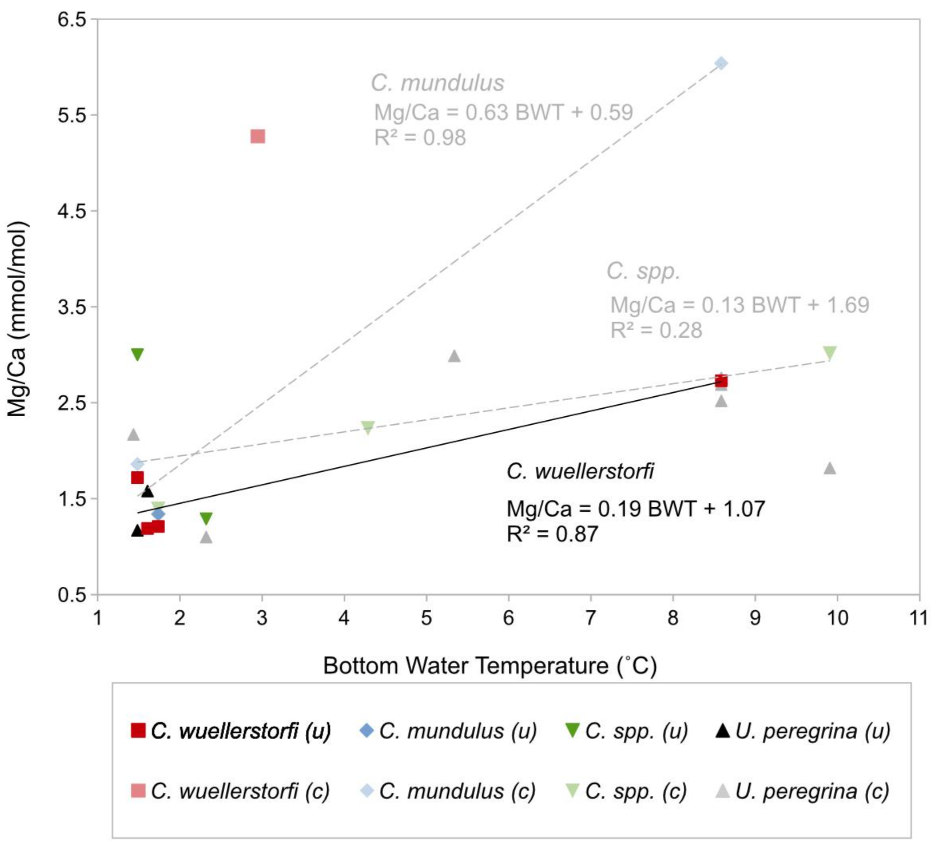

Figure~~.~~ 9.~~:~~ Mg/Ca ratios of *Cibicidoides spp*., *~~Cibicidoides~~ C. wuellerstorfi*, *~~Cibicidoides~~ C. mundulus* and *~~Uvigerina~~ U. peregrina* over bottom water temperature (BWT). ~~Grey~~Opaque colours: Measurements with suspected significant contamination (c). ~~Black~~Solid colours: uncontaminated/minor contamination based on contamination thresholds (0.1 mmol mol^{-1}~~mmol/mol F~~ Fe/Ca, 0.4 mmol mol^{-1}~~mmol/mol A~~ Al/Ca and 0.1 mmol mol^{-1}~~mmol/mol M~~ Mn/Ca)~~)~~ and correlations with Mg/Ca (uncontaminated samples indicated by (u). There are several data points where presence of contamination is ambiguous - see discussion. Black trendline represents Mg/Ca-BWT linear correlation in *C. wuellerstorfi* (four samples with minor contamination), grey trendlines represent tentative Mg/Ca-BWT linear correlations in *C. mundulus* and *Cibicidoides~~.~~ spp*. respectively (contaminated and uncontaminated samples included).

4. DISCUSSION

4.1. Mg/Ca ~~values~~ ratios in *Cibicidoides:* data quality and core top calibrations

All samples of *Cibicidoides* except for one have Mn/Ca ratios below the threshold for contamination (<0.1 mmol mol^{-1}) and no correlation with Mg/Ca ratios, suggesting no or insignificant Mn-oxide coatings (Hasenfratz et al., 2017). Based on silicate contamination indicated by Fe/Ca and Al/Ca ratios being significantly above the contamination threshold, six samples were excluded (three *Cibicidoides~~.~~ spp.*, two *C. ~~ibicidoides~~ mundulus* and one *C. ~~ibicidoides~~ wuellerstorfi* samples) (Table ~~3~~2). When plotted at the genus level, *Cibicidoides* ~~data~~ show no correlation between Fe/Ca or Al/Ca ratios and Mg/Ca ratios (Fig.~~ure~~ 6a-b) supporting the notion of no silicate contamination, amid this strategy being in line with previous approaches (e.g. Elderfield et al. 2006, Healey et al., 2008). When plotted at a species level, however, there is a strong correlation (~~r^2~~r^2=0.94) between Fe/Ca and Mg/Ca ratios for *C. ~~ibicidoides~~ wuellerstorfi* data (Fig. A1 in Appendix A ~~Fig.ure A1 in Appendix A~~) which suggests silicate contamination. The indicated contamination levels are small in most cases with Fe/Ca ratios below 0.25 mmol mol^{-1}. It is difficult to assess how much this small contamination has affected the Mg/Ca data. If the increase in Mg/Ca ratios from silicate contamination is within the uncertainty of Mg/Ca ratio determinations (~0.03 mmol mol^{-1}) this can be neglected.

We therefore used the Mg/Ca ratios of four *C.* ~~*ibicidoides*~~ *wuellerstorfi* samples with Fe/Ca below 0.25 mmol mol^{-1} to establish a Mg/Ca BWT relationship (Table 3~~2~~, Fig.~~ure~~ 9).

There are two ~~abnormally~~ anomalously high Mg/Ca ratios measured in *C.* ~~*ibicidoides*~~ *mundulus* (6.04 mmol mol^{-1}) and *C.* ~~*ibicidoides*~~ *wuellerstorfi* (5.28 mmol mol^{-1}; Table 3~~2~~) compared to Mg/Ca ratios in some studies (Elderfield et al., 2006; Rosenthal 1997) but within range of Mg/Ca ratios in other reports (Lear 2002; Rosenthal 1997). The *C. mundulus* sample with a Mg/Ca ratio of 6.04 mmol mol^{-1} shows a broadly similar Fe/Ca ratio but a significantly higher Al/Ca ratio (2.66 mmol mol^{-1}) than other measurements from the genus *Cibicidoides* (Al/Ca ratios ranging from 0.21 to 0.57 mmol mol^{-1}; Table 3~~2~~).~~-~~ It is uncertain whether the high Mg/Ca ratio is a result from silicate contamination or is due to another Mg bearing contaminant also high in Al. The Mn/Ca ratio in this sample is low (0.01 mmol mol^{-1}) indicating no presence of Mn-oxide coatings.

The *C. wuellerstorfi* sample with a Mg/Ca ratio of 5.28 mmol mol^{-1} does not have significantly higher Al/Ca, Fe/Ca or Mn/Ca ratios compared to ~~other~~ samples of *Cibicidoides spp.* suggesting limited contamination. ~~but has significantly~~ The low~~less~~ Ca concentration (3.99 ppm~~ compared to 14.42 to 75.62 ppm~~) could~~. The results from Experiment 3 implied a minimum concentration for Ca around 15 ppm for reliable Mg/Ca measurements. In this sample, the Ca concentration is significantly lower than the threshold which could be responsible for the abnormally high Mg/Ca ratio.~~ suggest the high Mg/Ca ratios are due to ~~The low Ca content could be due to~~calcite dissolution from chemical cleaning. However, low Ca concentrations could also be due to ~~-~~sample loss in crushing or~~,~~ sample loss during transfer in chemical cleaning. Whilst efforts have been made to minimise sample loss from crushing (using individual crushing), sample loss during transfer in chemical cleaning (using MilliQ to rinse brush) and when rinsing samples during MilliQ and methanol rinses (not agitating samples when using vacuum), it is not possible to eliminate sample loss entirely. This is one of the major limitations with the methodology and should be considered a significant source of uncertainty. This sample was excluded from the Mg/Ca ratio – BWT calibration model. ~~or calcite dissolution from chemical cleaning.~~

The Mg/Ca ratio - BWT relationship of *C.* ~~*ibicidoides*~~ *wuellerstorfi* $Mg/Ca = 0.19 \pm 0.02 * BWT + 1.07 \pm 0.03$, indicates increasing Mg/Ca ratios with increasing temperature, and is broadly consistent with previous studies (Fig.~~gure~~ 10, Healey et al., 2008; Lear et al., 2002) although there is only one data point reflecting the high temperature end of our calibration range of 3-8 ˚C. The temperature sensitivity of *C.* ~~*ibicidoides*~~ *wuellerstorfi* in this study (19% increase per 1˚C) is lower than ~~in~~ Elderfield et al. (2006, 46% and 52% increase per 1˚C) ~~)~~and Healey et al. (2008, 30%~~);~~ ~~19%~~ increase per 1˚C)~~ change in temperature compared to 30% (Healey et al., 2008) and 46 and 52% (Elderfield et al., 2006), see Fig. 10~~. Also, two Mg/Ca ratios (ignoring a probable outlier with a high Mg/Ca ratio) at lower temperatures (<2˚C) are within the data range of both, the southeast Indian Ocean calibration of *C. wuellerstorfi* by Healey et al. (2008) and the Southwest Indian Ocean calibration of *C. wuellerstorfi* by Elderfield et al. (2006), ~~-~~but are higher than the Mg/Ca ratios of *C. wuellerstorfi* from the Somali basin (Elderfield et al., 2006; ~~included in Elderfield 2006 data in~~ Fig.~~ure ???~~10~~1~~). ~~-~~These high Mg/Ca values do, however, fall within the range of values found in *C.* ~~*ibicidoides*~~ *wuellerstorfi* from the Atlantic Ocean. There is a discussion surrounding relatively unmixed NADW crossing the Davie Ridge into the Somali basin (van Aken et al., 2004). Our core-top sample set is in the flow path of NADW, supporting the notion our high Mg/Ca ratios reflecting NADW specific water properties. Firm conclusions are hampered by the limited sample size in our *C.* ~~*ibicidoides*~~ *wuellerstorfi* data set. If correct, however, changing water masses in a given location, may add additional uncertainties to BWT reconstructions.

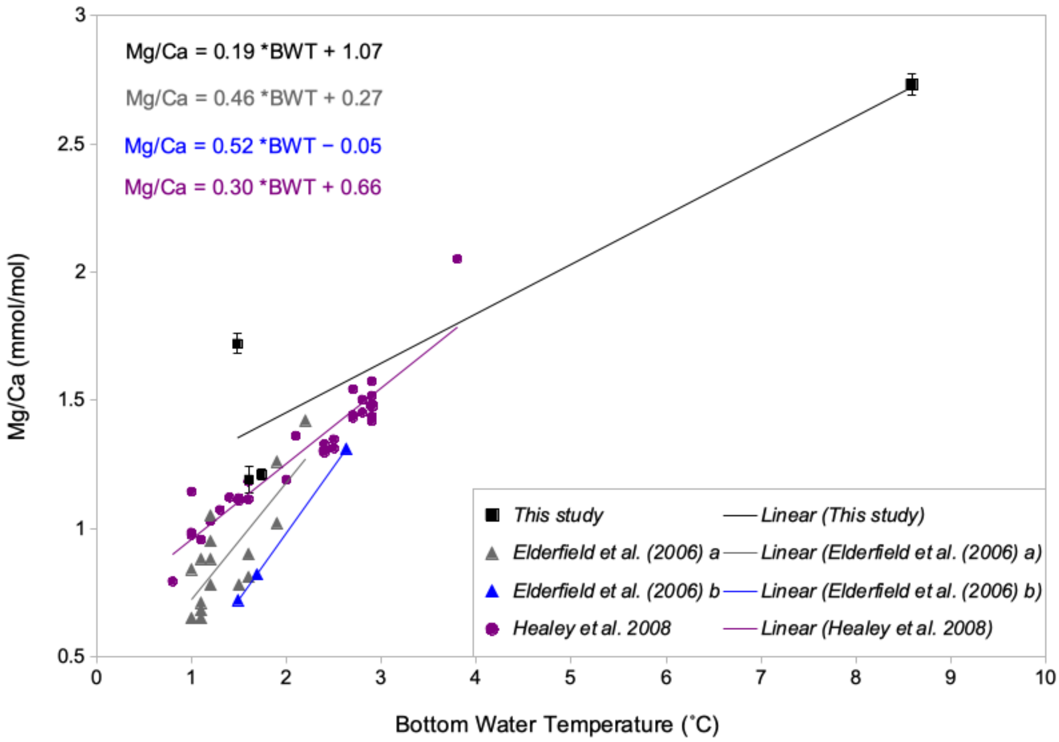

Figure~~.~~ 10.~~:~~ Mg/Ca – BWT calibrations of *C. ~~ibicidoides~~ wuellerstorfi* from various studies; in black: this study with error bars showing standard deviation, purple: S.~~-~~E. Indian Ocean from Healey et al. (2008), grey: S.~~-~~W. Indian Ocean from Elderfield et al. (2006) ~~-~~and blue: Somali basin from Elderfield et al. (2006).

Previous studies have used both linear and exponential regressions to describe the temperature dependence of Mg/Ca ratios (e.g. Healey et al., 2008; Lear et al., 2002, Martin and Lea, 2002; Elderfield et al., 2006) with some studies suggesting the latter being preferable at low temperatures and over narrow temperature ranges (Healey et al., 2008; Stirpe et al., 2021). The small sample size in our study hampers assessment of the better regression strategy. The generally good fit with the linear regression in Healey et al. (2008) and the data ranges in Lear et al. (2002), support the notion of our Indian Mg/Ca calibration being broadly correct.

Two out of three Fe/Ca and Al/Ca ratios for *C. ~~ibicidoides~~ mundulus* are significantly above contamination thresholds (Table 3~~2~~). In the absence of a correlation with Mg/Ca ratios (Fig.~~ure~~ 6a-b) all three Mg/Ca ratios were tentatively plotted and compared to existing *C. ~~ibicidoides~~ mundulus* core-top calibrations (Fig.~~ure~~ 11). The estimated Mg/Ca ratios in the temperature range of 1-2˚C ~~is~~ are within the range of Healey et al. (2008). One of the data points seems sufficiently cleaned whilst the second does not, based on low and high Al/Ca and Fe/Ca ratios, respectively. Because both values lie within the range of data provided by Healey et al. (2008) this suggests high estimates of Fe/Ca and Al/Ca ratios being a result of a non-Mg bearing contaminant (not silicate), supported by absent correlations between Al/Ca or Fe/Ca with Mg/Ca (Fig.~~ure~~ 6a-b). Alternatively, this could suggest increased Mg/Ca ratios that may be interpreted as silicate contamination but are within the natural variation of Mg/Ca ratios in *C. ~~ibicidoides~~ mundulus*.

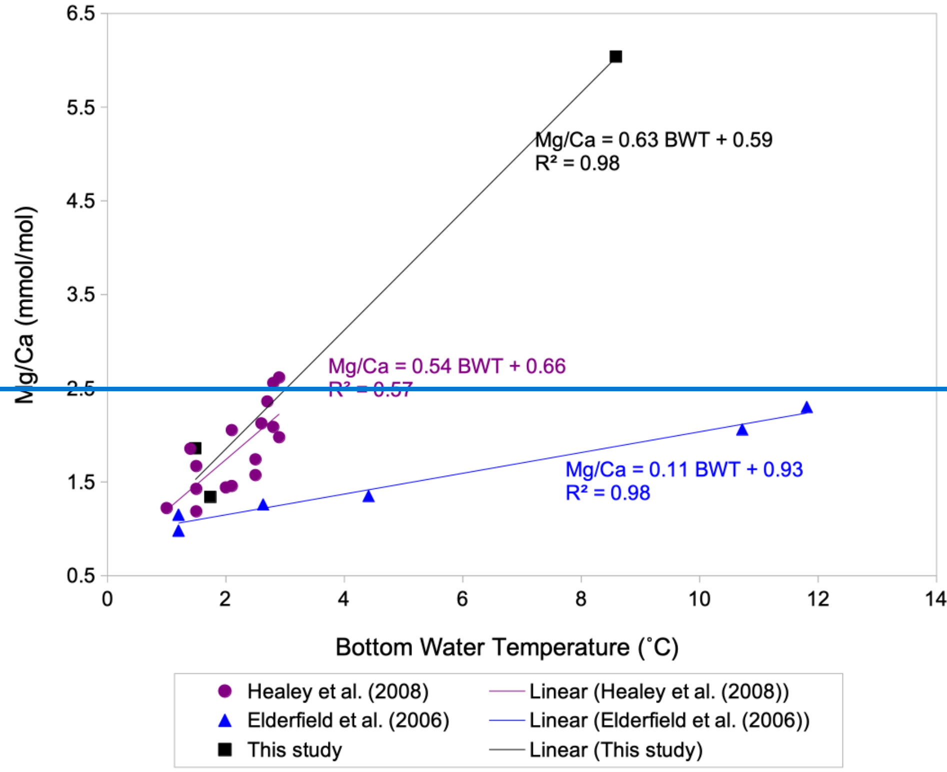

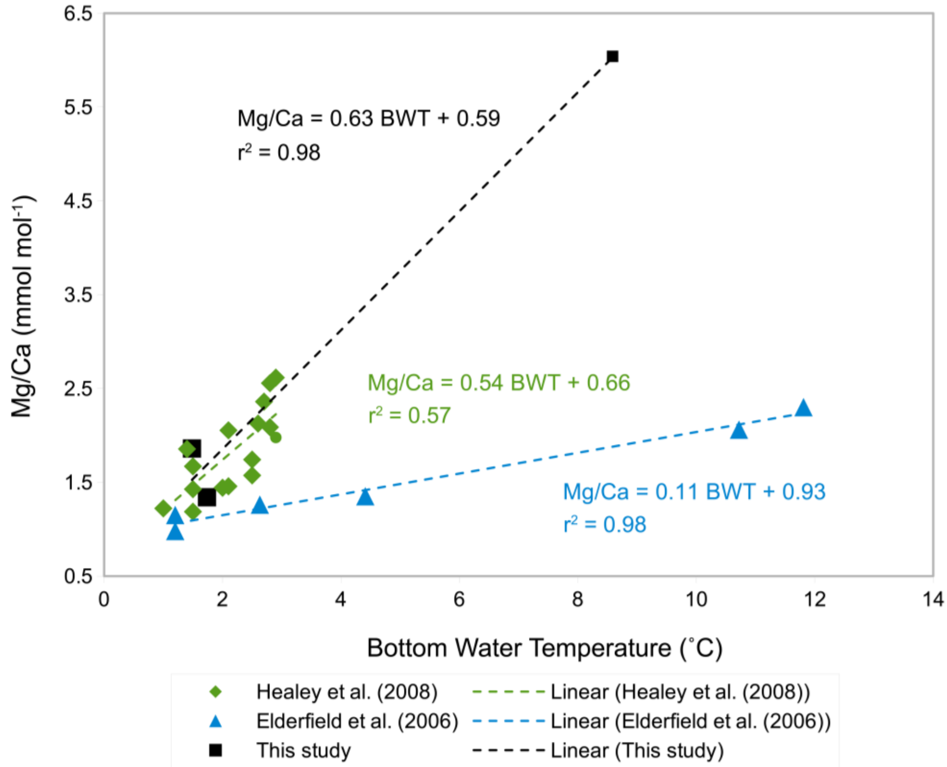

Figure~~.~~ 11.~~:~~ Tentative Mg/Ca – BWT calibration of ~~*Cibicidoides*~~ *C. mundulus* in this study (black squares) compared to core-top calibrations ~~in *Cibicidoides mundulus*~~ by Healey et al. (2008) (~~purple~~green rhombs) and Elderfield et al. (2006) (light blue triangles).

The linear relationship of the three Mg/Ca ratios of *C.* ~~*ibicidoides*~~ *mundulus* in Fig. 11 closely resembles the linear relationship derived from data by Healey et al. (2008) from core-top estimates from the Atlantic, Pacific and Indian Ocean combined ~~(Figure 11)~~ although the reliability in our study is limited by only three datapoints and only one value at high temperatures.~~-~~ Our and

Healey et al.'s (2008) calibrations differ from the S~~-~~W Indian Ocean calibration from Elderfield et al. (2006) with the reasons for this discrepancy being unclear.

4.2. Mg/Ca ratios in *Uvigerina peregrina*

Our results for *U.* ~~*vigerina*~~ *peregrina* show that Mg/Ca ratios in nine samples of *U.* ~~*vigerina*~~ *peregrina* range from 1.10 to 2.99 ± 0.02 mmol mol^{-1} (Table 3~~2~~) covering a depth range of 370-3323 m (Table 1). These Mg/Ca ratios are higher than values reported by Stirpe et al. (2021) ranging from 0.68 to 1.50 mmol mol^{-1} covering a depth range of 663 to 4375 m. In our data set, 7 out of 9 samples have Fe/Ca ratios above the contamination threshold (>0.1 mmol mol^{-1}) and correlate positively with Mg/Ca ratios (~~r^2~~r^2=87, Fig.~~ure~~ 7a) suggesting silicate contamination. Al/Ca ratios in all samples are above the contamination threshold (>0.4 mmol mol^{-1}) and correlate with Mg/Ca ratios (~~r^2~~r^2=0.66, Fig.~~ure~~ 7b). These findings suggest silicate contamination being reflected in our high Mg/Ca ratios. Mn/Ca ratios in all samples are below the contamination threshold (<0.1 mmol mol^{-1}) which ~~suggest~~ supports the notion of ~~no presence of~~ Mn-oxide coatings being absent (Fig.~~ure~~ 7c).

To investigate if the high Mg/Ca ratios are indeed a result of silicate contamination these were plotted versus bottom water temperatures and compared to previous studies (Fig.~~ure~~ 12). Only two samples of *U.* ~~*vigerina*~~ *peregrina* are below the contamination threshold of Fe/Ca ratios (<0.1 mmol mol^{-1}, Elderfield et al., 2010). These map onto the relationship of *U.* ~~*vigerina*~~ *peregrina* by Elderfield et al. (2006). Most of the samples ~~with Mg/Ca ratios~~ that were suggested to be silicate contaminated ~~are~~show, as expected, significantly higher Mg/Ca ratios than previous estimates (Fig. ~~ure~~ 12), up to 1.5 mmol mol^{-1} higher than in the relationship of Elderfield et al. (2006). This supports the notion that Fe/Ca and Al/Ca ratios well above the contamination threshold indeed identify samples with contamination that bias the Mg/Ca ratios.

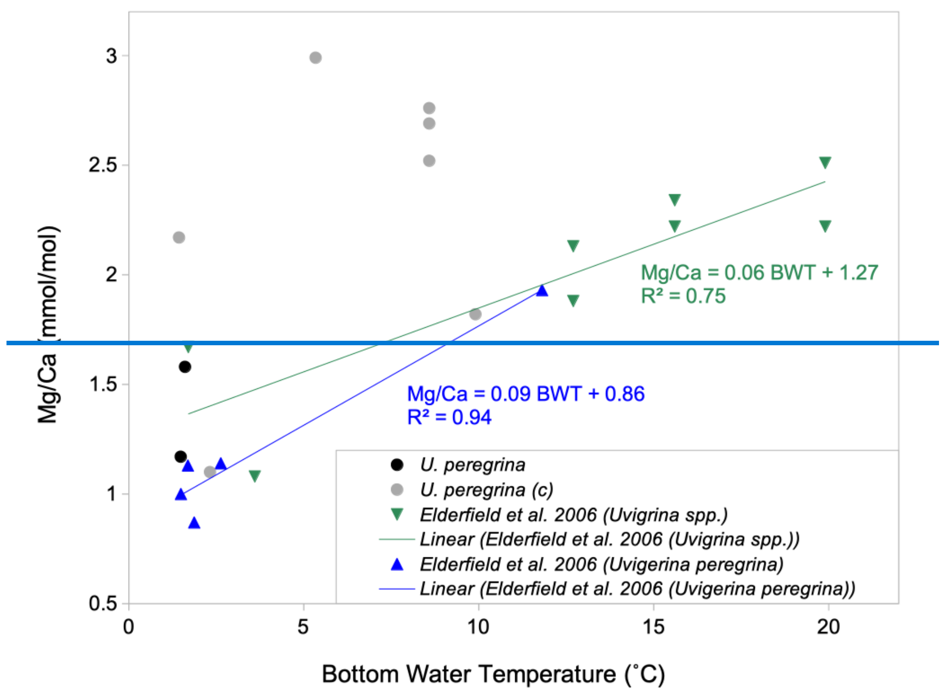

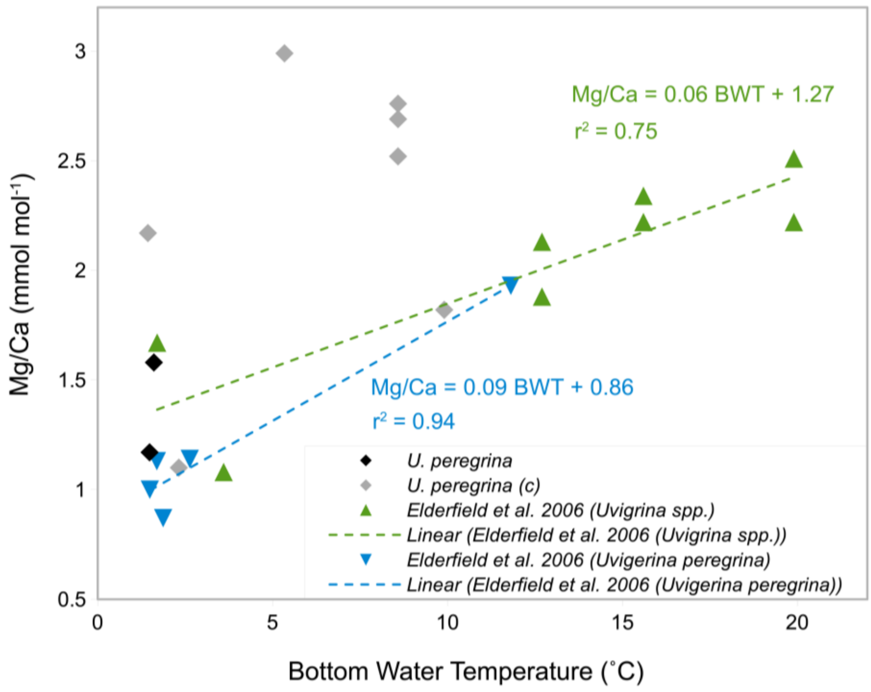

Figure~~.~~ 12 Mg/Ca – BWT calibration of ~~*Uvigerina*~~ *U. peregrina* in this study (~~circles, grey~~grey rhombs: contaminated, black rhombs: uncontaminated) compared to Elderfield et al. (2006) core-top calibrations of light blue triangles: ~~*Uvigerina*~~ *U. peregrina* and green triangles: *Uvigerina spp*.

Mg/Ca ratios measured in *U. ~~vigerina~~ peregrina* in a previous study (Yu et al., 2007) showed no significant difference between cleaning method using weaker reductive cleaning reagents and oxidative cleaning only, in contrast to Mg/Ca ratios measured in *C. ~~ibicidoides~~ wuellerstorfi* and *C. ~~ibicidoides~~ mundulus* showing a significant difference (Yu et al., 2007). The clear difference in contamination, between *Cibicidoides spp*. (Fig. ~~ure~~ 6) and *U. ~~vigerina~~ peregrina* (Fig. ~~ure~~ 7) despite using the same cleaning procedure, supports the findings in ~~(~~Yu et al., (2007), which suggest different rigour might be required for different species (please see section 4.6 on variable degree of contamination).

4.3. Sufficient cleaning of Mn-oxide coatings

~~While~~ Although the cleaning procedure ~~used in this study~~ by Barker et al. (2003) has been widely used (e.g. Elderfield et al., 2006; Elderfield et al., 2010, Elmore et al., 2015), the removal of ~~inefficient removal of~~ Mn-Mg coatings ~~has~~ is~~been~~ inefficient in some cases~~observed~~ (Hasenfratz et al., 2017; Pena et al., 2005). The Mn-oxide coatings which are found on the inner shells of foraminifera can cause increased Mg/Ca ratios and only the reductive cleaning procedure satisfactorily removes this (Pena et al., 2005). Where Mn/Ca ratios are below 0.2 mmol mol^{-1}, it entails a small increase in Mg/Ca ratios that is within the uncertainty of Mg/Ca ratio determination and therefore can be considered insignificant (Hasenfratz et al., 2017). All but one core-top sample have Mn/Ca ratios below 0.2 mmol mol^{-1} (Fig.~~ure~~ 6 and 7, Table 3~~2~~). This suggests the reductive cleaning step was not needed for samples analysed in this study, and therefore it is assumed the 'Mg cleaning procedure' utilised in this study is more suitable than the 'Cd cleaning procedure'.

4.4. Inefficient cleaning of silicate contaminants

The high Fe/Ca ~~and~~ as well as the high Al/Ca ratios in most samples of all species used here (Table 3) indicate inefficient removal of silicate contaminants, suggesting that the number of rinse/ultrasonication repetitions of the Barker et al. (2003) procedure is inadequate. ~~all but two samples of the *Uvigerina peregrina* and six samples of *Cibicidoides spp*. (Table 2) suggest~~

~~inefficient removal of silicate contaminants, implying that the number of rinse/ultrasonication repeats was insufficient for efficient cleaning of samples despite following the Barker et al. (2003) procedure.~~ Increasing the number of rinse/ultrasonication repeats further (from four to five) entails the risk of considerable calcite dissolution which may lower the Mg/Ca ratios (Marr et al. 2013). There is probably a threshold at which tests are thoroughly cleaned and tests dissolve. A stepwise leaching test series could be used to investigate the rigour needed to optimise cleaning whilst avoiding sample loss in the process. Due to time limitations, however, this was not possible. If the methodology needs to be adapted to specific foraminifera species this highly limits the comparability between studies investigating different species from different core locations.

4.5. Species specific differences in silicate contamination

The range of Fe/Ca ratios in *U.~~vigerina~~ peregrina* was wider~~higher~~ (0.02~~43~~ to 2.04 mmol mol^{-1}) than in *C.~~ibicidoides~~ wuellerstorfi* (0.13 to 0.35 mmol mol^{-1}; Table 3). This is consistent with Elmore et al. (supplementary material, 2015) reporting Fe/Ca ratios below 0.1 mmol mol^{-1} in *U.~~vigerina~~ peregrina* compared to Fe/Ca ratios ~~below 0.04 mmol mol^{-1}~~ in *C.~~ibicidoides~~ wuellerstorfi*~~.~~ below 0.04 mmol mol^{-1}. Both ranges are below the contamination threshold (0.1 mmol mol^{-1}) in contrast to ranges reported in this study. Elmore et al. (2015) also used the procedure of Barker et al. (2003). Samples containing *G. ruber* from ~~the~~ core NIOP 9~~0~~29~~5~~ were included in the analysis of core-tops and used as a control to monitor cleaning efficiency. On average ~~the~~ *G. ruber* contained Fe/Ca, Al/Ca and Mn/Ca ratios of 0.18, 0.60 and 0.15 mmol mol^{-1} (~~see Table A2 in~~ Table A4 in Appendix A~~Appendix A Table A4~~). Both average Fe/Ca ratios and average Al/Ca ratios in ~~samples of~~ *G. ruber* from NIOP929 ~~that were~~ analysed in runs along with *U.~~vigerina~~ peregrina* (0.31 and 1.09 mmol mol^{-1}) were higher than that of ~~the Fe/Ca and Al/Ca ratios in samples of~~ *G. ruber* that were analysed in runs alongside *Cibicidoides spp*. (0.13 and 0.26 mmol mol^{-1}~~Table A2 in A~~; ~~Appendix A~~ Table A4 in Appendix A). Since the same procedure was followed, the difference could point to an issue in the repeatability of the cleaning procedure, i.e. build-up of gas bubbles in hot water bath during the oxidative step, insufficient crushing prior to cleaning or different quantities~~y~~ of MilliQ water and methanol removed in between rinses affecting efficiency of contaminants being removed in every rinse. Alternatively, the different contamination levels can also result from ~~might be due~~ different samples ~~having~~ from core NIOP929 used due ~~been used as a result of~~to insufficient specimens of *G. ruber* ~~being contained~~ found ~~in~~ within a single sample. ~~from core NIOP929.~~

4.6. Variable initial degree of contamination

The degree of contamination of tests depends on factors including sediment composition, sedimentation rates, oxygen concentrations, core depth, water depth, and morphology (Barker et al., 2003; Ni et al., 2020; Pena et al., 2005). While foraminiferal tests that are well preserved and show no to minor signs of contamination were selected for analysis, the condition of specimens selected vary (qualitative observations of samples described in Appendix C). If *U. peregrina*, as an endobenthic species is subject to more contact with surrounding sediment particles than *C. wuellerstorfi* this could explain higher contamination in *U. peregrina*. Also, the surface of tests of *C. wuellerstorfi* is relatively smooth compared to the irregular surface of *U. peregrina* tests, entailing a larger surface area compared to *C. wuellerstorfi* which in turn increases the probability of contaminants sticking onto tests of *U. peregrina*.

~~The degree of contamination of tests depends on factors including sediment composition, sedimentation rates, oxygen, depth in core, depth, and morphology (Barker et al., 2003; Ni et al., 2020; Pena et al., 2005). While foraminiferal tests that are well preserved and show no to minor signs of contamination were selected for analysis, the condition of core-top samples vary (qualitative observations of samples described in Appendix C). If *Uvigerina peregrina*, as an endobenthic species is subject to more contact with surrounding sediment particles than *Cibicidoides wuellerstorfi* this could explain higher contamination in *Uvigerina peregrina*. Also, the structure of the test wall may lead to different susceptibilities for contamination. By comparison,~~

~~the surface of tests of *Cibicidoides wuellerstorfi* are relatively smooth. The surfaces of *Uvigerina peregrina* tests, however, are irregular, entailing a larger surface area compared to *Cibicidoides wuellerstorfi* which in turn increases the probability of contaminants sticking onto tests of *Uvigerina peregrina*.~~

4.7. Different depositional environment

Barker et al. (2003) suggest samples from regions of higher clay content require more rigorous cleaning. This study benefits from using core top samples from a relatively localised area (within a radius of 1˚E and S – see Fig. 1) in comparison to previous studies based on more widely distributed samples (e.g. Elderfield et al., 2006). Despite the close proximity of our samples, different depositional environments likely exist in our core top sample set. To investigate the correlation between depositional environment and silicate contamination, Fe/Ca ratios and Al/Ca ratios over depth were plotted (Fig. 8). There is an inverse correlation between Fe/Ca ratios and Al/Ca ratios with depth in *U. peregrina* samples (Fig. 8) and samples at depths >2000 m having significantly lower Fe/Ca ratios and Al/Ca ratios. Our core top transect is located close to the Rovuma River, implying lithogenic material deposited near its mouth. The redistribution of these sediments may well have affected the upper parts more than the deeper parts of the continental slope in our study area (compare van der Lubbe et al. (2014), which is probably reflected in the higher contamination level at shallower depths).

~~Barker et al. (2003) suggest samples from regions of higher clay content require more rigorous cleaning. This study benefits from using core-top samples in a nearby region in contrast to previous studies (e.g. Elderfield et al., 2006). While core-tops are located within a nearby region they cover a depth range of 370 m to 3323 m and are thereby in different depositional environments. Barker et al. (2003) suggest samples from regions of higher clay content require more rigorous cleaning. To investigate correlation between depositional environment and silicate contamination Fe/Ca, Al/Ca ratios over depth were plotted (see Figure 8. There is an inverse correlation between Fe/Ca and Al/Ca ratios with depth in *Uvigerina peregrina* samples (Figure 7, and samples at depths >2000 m have significantly lower Fe/Ca and Al/Ca ratios. Our core top transect is located close to the Rovuma River, implying lithogenic material deposited near its mouth. The redistribution of these sediments may well have affected the upper parts more than the deeper parts of the continental slope in our study area, which is probably reflected in the higher contamination level at shallower depths.~~

4.8. Relative impact of contamination

The Mg/Ca ratios are typically lower in benthic foraminifera compared to planktic foraminifera and therefore the relative impact of contamination in benthic foraminifera is larger (de Vielliers et al., 2002). While contamination thresholds following previous benthic foraminifera core-top studies have been used here, a lower contamination threshold for benthic foraminifera should be used to minimise the relatively higher uncertainty for benthic Mg/Ca ratios (Hasenfratz et al., 2017). Different species of benthic foraminifera show different temperature sensitivities, i.e. the relative change in calcite Mg/Ca ratios compared to changes in temperature (Gussone et al., 2016). The impact of contamination on Mg/Ca-based temperature estimates varies with the temperature sensitivity in different foraminifera species (*U. peregrina* > *Cibicidoides spp*.). *Cibicidoides spp*. has previously been shown to have different temperature sensitivities at different temperature ranges (Elderfield et al., 2006). The temperature sensitivity of *Cibicidoides spp*. including *C. mundulus* and *C. wuellerstorfi* is higher at temperatures above 3˚C and therefore the relative impact is ~~stronger~~smaller in temperatures above 3˚C.

~~The Mg/Ca ratios are typically lower in benthic foraminifera compared to planktic foraminifera and therefore the relative impact of contamination in benthic foraminifera is larger (de Vielliers et al., 2002). While contamination thresholds following previous benthic foraminifera core-top studies have been used here, a lower contamination threshold for benthic foraminifera should be used to minimise the relatively higher uncertainty for benthic Mg/Ca ratios (Hasenfratz et al., 2017). Different species of benthic~~

~~foraminifera show different temperature sensitivity, i.e. the relative change in calcite Mg/Ca ratios to changes in temperature (Gussone et al., 2016). The accuracy of Mg/Ca-based temperature estimates in foraminifera species with higher temperature sensitivity (*Uvigerina peregrina* > *Cibicidoides spp.*) is thus more impacted by contamination. *Cibicidoides spp.* has previously been shown to have different temperature sensitivity at different temperature ranges (Elderfield et al., 2006). Temperature sensitivity of *Cibicidoides spp.* including *Cibicidoides mundulus* and *Cibicidoides wuellerstorfi* is higher at temperatures above 3˚C and therefore the relative impact is stronger in temperatures above 3˚C.~~

4.9. Different contamination thresholds

Different studies have used different indicators and thresholds to monitor silicate contamination and Mn-oxide coatings. Barker et al. (2003) consider correlations between Mg/Ca ratios and Fe/Ca and/or ~~,~~ Al/Ca ratios ~~with Mg/Ca ratios~~ as indicators of silicate contamination. Elderfield et al. (2010) have used contamination thresholds of 0.4, 0.1 and 0.1 mmol mol^{-1} of Al/Ca, Fe/Ca and Mn/Ca ratios, respectively, as indicators of contamination, ~~-~~but~~,~~ also state~~s~~ because of difficulties with the precision of Al concentrations, the Mg/Ca ratios were not excluded based on high Al/Ca ratios alone. Yu and Elderfield (2008) used correlations between Al/Ca and Mn/Ca ratios with Mg/Ca ratios to assess contamination. Capelli et al. (2005) have used Al/Ca ratios <1 mmol mol^{-1} and correlation with Mg/Ca ratios to identify silicate contamination. In contrast, St~~r~~irpe et al. (2021) have used more strict thresholds of 0.0952, 0.0296 and 0.0189 µmol mol^{-1} of Al/Ca, Fe/Ca and Mn/Ca ratios, respectively. While the most common contamination is based on correlations with Fe/Ca, Al/Ca and Mn/Ca, the outlined differences cause uncertainty when comparing results between studies. When only using correlations between Fe/Ca, Al/Ca ratios and Mg/Ca ratios to assess silicate contamination, no samples of *Cibicidoides spp.* in this study would have been tagged as contaminated. However, when correlations are used in combination with the contamination thresholds, about half of the samples indicate silicate- ~~contamination~~ or other contamination. Also, when assessing correlations at species level, i.e. ~~—~~*C.* ~~*ibicidoides*~~ *wuellerstorfi*, there is a strong correlation between Fe/Ca and Mg/Ca ratios (~~Figure 1A in Appendix A~~ Fig. 1A in Appendix A, excluding *Cibicidoides spp.* and *C.* ~~*ibicidoides*~~ *mundulus* which were analysed in the same run). The species difference could be due to morphological features of *C.* ~~*ibicidoides*~~ *wuellerstorfi* that allow more silicate contaminants to be trapped. On the other hand, if the lower contamination thresholds of Stirpe et al. (2021) are used, all Mg/Ca ratios of this study are suggested to be contaminated with both silicate and Mn-oxide coatings. Correlation between Fe/Ca, Al/Ca and Mn/Ca with Mg/Ca helps identify contaminants that also contain Mg (most notably silicate and Mn-oxide coatings) and are therefore relevant for determining calcite Mg/Ca ratios. Excluding samples based on strict contamination thresholds for Fe, Al and Mn, without considering correlations to Mg/Ca ratios risks excluding many samples that have minor contaminants which do not affect Mg/Ca ratios. These measurements could still prove a reliable estimate of Mg/Ca ratios. Still, any presence of contamination is a concern. Even if it does not produce~~s~~ inaccurate Mg/Ca ratios (in the case that the contaminant does not contain Mg), it introduces uncertainties. The inconsistencies between studies and the uncertainties ~~would~~ used could be resolved by further examination of appropriate contamination thresholds ~~to be used~~. For example, elemental analysis of a sample containing visible contamination from every core sample that foraminifera tests are picked from could be introduced in the methodology. This would help assess the identified contamination effect on Mg/Ca ratios measured in the foraminifera tests from a particular sample and specify contamination thresholds that are specific to each sample. Because the degree of contamination effect depends on factors such as average Mg/Ca ratios and temperature sensitivity a more appropriate contamination threshold should be species specific and at least ~~specific~~ detailing ~~to~~ benthic versus planktic foraminifera differences ~~/planktic~~ since average Mg/Ca ratios are significantly lower in benthic species (Hasenfratz et al., 2017).

5. SUMMARY AND CONCLUSION

Designed to optimise the relationship between sample cleaning involved in Mg/Ca thermometry and sample loss during the procedure, in experiments 1-3 varying methanol and ultra-pure water rinses were used and clearly show a substantial effect on the level of silicate contamination. These experiments showed that the best cleaning method for our study was that of Barker et al. (2003).

The core-top calibration for *C. ~~Cibicidoides~~ wuellerstorfi* in this study, only including four samples, is broadly in line with published data, although there is only one data point in our study at the high temperature end.

Contamination is a general problem. Despite using an established method (Barker et al. 2003), in particular~~,~~ *U. ~~vigerina~~ peregrina* displayed high levels of remanent contamination. The *U. ~~vigerina~~ peregrina* Mg/Ca ratios also indicate that the contamination indicating thresholds have generally been correct in identifying samples with silicate contamination.

There are several potential sources of error for Mg/Ca ratios including the carbonate ion effect, diagenetic effects, seawater Mg/Ca variability, and vital effects. The main limitation in the use of Mg/Ca as a paleothermometer is a general lack of understanding of benthic foraminiferal Mg incorporation and the relative impact of environmental factors, biogenic controls and diagenetic effects. It is possible that species specific cleaning protocols are needed to improve comparability of data between studies.

6. Competing Interests

S. Jung is co-editor of the special issue dedicated to Dick Kroon and will not be involved in the handling of this manuscript. The other authors declare that they have no conflict of interest.

7. Author contribution

The research was conceptualised by S. Jung and V. Larsson. V. Larsson designed, carried out experiments, conducted data analysis, visualisation and prepared the original manuscript. This was done with supervision and validation input from S. Jung. S. Jung ~~prepared the final manuscript with input from~~and V. Larsson jointly prepared the final manuscript.

8. Acknowledgments

The authors thank Dr. Laetitia Pichevin for advice on experimental design and statistical analysis, Prof. Raja Ganeshram for advice on the Mg/Ca cleaning methodology and the PGR staff in the Geoscience Department at The University of Edinburgh for providing administrative help.

9. REFERENCES

Anand, P., Elderfield, H., & Conte, M.H. (2003). Calibration of Mg/Ca thermometry in planktonic foraminifera from a sediment trap time series. Paleoceanography, 18(2). Retrieved from https://doi.org/10.1029/2002PA000846

Balsam, W. L., Gary, A. C., & Williams, D. F. (1986). Morphology and time/depth distribution of Uvigerina peregrina: continental slope, Eastern Margin, United States.

Barker, S., Cacho, I., Benway, H., & Tachikawa, K. (2005). Planktonic foraminiferal Mg/Ca as a proxy for past oceanic temperatures: a methodological overview and data compilation for the Last Glacial Maximum. Quaternary Science Reviews, 24(7), 821–834. Retrieved from https://doi.org/10.1016/j.quascirev.2004.07.016

Bell, D. B., Jung, S. J. A., Kroon, D., Lourens, L. J., and Hodell David, A.: Local and regional trends in Plio-Pleistocene d18O records from benthic foraminifera, Geochem. Geophys. Geosyst., 10.1002/2014GC005297, 2014.

Bentov, S., & Erez, J. (2006). Impact of biomineralization processes on the Mg content of foraminiferal shells: A biological perspective. Geochemistry, Geophysics, Geosystems : G3, 7(1). Retrieved from https://doi.org/10.1029/2005GC001090

Bickert, T. and Mackensen, A.: Last Glacial to Holocene changes in South Atlantic deep water circulation, in: The South Atlantic in the late Quaternary: Reconstruction of material budgets and current systems, edited by: Wefer, G., Mulitza, S., and Ratmeyer, V., Springer Verlag, Berlin, Heidelberg, New York, Tokyo, 671-695, 2003.

Birch, H., Coxall, H. K., Pearson, P.N., & Kroon, D. (2013). Planktonic foraminifera stable isotopes and water column structure: Disentangling ecological signals. Marine Micropaleontology, 101, 127–145.

Blunier, T., Chappellaz, J., Schwander, J., Clausen, H., Hammer, C. U., & Johnsen, S. (1998). Asynchrony of Antarctic and Greenland climate change during the last glacial period. Nature, 349, 739–743.

Boyle, E. A., & Keigwin, L. D. (1985). Comparison of Atlantic and Pacific paleochemical records for the Last 215,000 years: Changes in deep ocean circulation and chemical inventories. Earth and Planetary Science Letters, 76, 135–150.

Brady, H. B., Parker, W. K., & Jones, T. R. (1888). On some foraminifera from the Abrolhos Bank. Transactions of the Zoological Society, London, 12, 40-47.

Branson, O., Redfern, S.A.T., Tyliszczak, T., Sadekov, A., Langer, G., & Elderfield, H. (2013). The coordination of Mg in foraminiferal calcite. Earth and Planetary Science Letters, 383. Retrieved from https://doi.org/10.1016/j.epsl.2013.09.037

Branson, O., Read, E., Redfern, S. A., Rau, C., & Elderfield, H. (2015). Revisiting diagenesis on the Ontong Java Plateau: Evidence for authigenic crust precipitation in Globorotalia tumida: Foram Dissolution and Reprecipitation. Paleoceanography, 30.

Broecker, W., Clark, E., McCorkle, D., Hajdas, I., & Bonani, G. (1999). Core top 14C ages as a function of latitude and water depth on the Ontong-Java Plateau. Paleoceanography, 14, 13-22.

Lo Giudice Cappelli, E., Regenberg, M., Holbourn, A., Kuhnt, W., Garbe-Schönberg, D., & Andersen, N. (2015). Refining C. wuellerstorfi and H. elegans Mg/Ca temperature calibrations. Marine Micropaleontology, 121, 70–84. [Online]

Clark, P.U., Pisias, N.G., Stocker, T.F., & Weaver, A.J. (2002). The role of the thermohaline circulation in abrupt climate change. Nature, 415(6874), 863-869.

Curry, W.B., Duplessy, J.C., Labeyrie, L.D., & Shackleton, N.J. (1988). Changes in the distribution of delta ^(13)C of deep water Sigma CO (sub 2) between the last glaciation and the Holocene. Paleoceanography, 3, 317-341.

Cushman, J.A. (1923). The Foraminifera of the Atlantic Ocean pt. 4: Lagenidae. Bulletin of the United States National Museum, (104), i-228.

de Villiers, S., Greaves, M., & Elderfield, H. (2002). An intensity ratio calibration method for the accurate determination of Mg/Ca and Sr/Ca of marine carbonates by ICP-AES. Geochemistry, Geophysics, Geosystems. doi:10.1029/2001gc000169

De Nooijer, L.J., Hathorne, E.C., Reichart, G.J., Langer, G., & Bijma, J. (2014). Variability in calcitic Mg/Ca and Sr/Ca ratios in clones of the benthic foraminifer Ammonia tepida. Marine Micropaleontology, 107, 32–43. [Online]

Downes, S.M., Bindoff, N.L., & Rintoul, S.R. (2010). Changes in the Subduction of Southern Ocean Water Masses at the End of the Twenty-First Century in Eight IPCC Models. Journal of Climate, 23(24), 6526-6541. Retrieved Oct 10, 2022, from https://journals.ametsoc.org/view/journals/clim/23/24/2010jcli3620.1.xml

Duplessy, J.-C., Duplessy, G.-J., Hayes, G., Labeyrie, M., Leclaire, J.-C., Duprat, J.-P., Pujol, E., Turon, M., & van Weering, E. (1988). Deep water source variations during the last climatic cycle and their impact on the global deepwater circulation. Paleoceanography, 3, 343-360.

Eggins, S.M., Sadekov, A., & De Deckker, P. (2004). Modulation and daily banding of Mg/Ca in Orbulina universa tests by symbiont photosynthesis and respiration: a complication for seawater thermometry? Earth and Planetary Science Letters, 225, 411–419. [Online]

Elderfield, H., Bertram, C. J., & Erez, J. (1996). A biomineralization model for the incorporation of trace elements into foraminiferal calcium carbonate. Earth and Planetary Science Letters, 142(3), 409–423.

Elderfield, H., & Ganssen, G. (2000). Past temperature and delta (super 18) O of surface ocean waters inferred from foraminiferal Mg/Ca ratios. Nature (London), 405, 442-445.

Elderfield, H., Yu, J., Anand, P., Kiefer, T., & Nyland, B. (2006). Calibrations for benthic foraminiferal Mg/Ca paleothermometry and the carbonate ion hypothesis. Earth and Planetary Science Letters, 250, 633–649.

Elderfield, H., Greaves, M., Barker, S., Hall, I. R., Tripati, A., Ferretti, P., Daunt, C. (2010). A record of bottom water temperature and seawater d18O for the Southern Ocean over the past 440kyr based on Mg/Ca of benthic foraminiferal Uvigerina spp. Quaternary Science Reviews, 29, 160–169.

Elmore, A., McClymont, E., Elderfield, H., Kender, S., Cook, M., Leng, M., Misra, S. (2015). Antarctic Intermediate Water properties since 400 ka recorded in infaunal (Uvigerina peregrina) and epifaunal (Planulina wuellerstorfi) benthic foraminifera. Earth and Planetary Science Letters, 428, 193-203. https://doi.org/10.1016/j.epsl.2015.07.013

Emiliani, C. (1955). Pleistocene temperatures. The Journal of Geology, 63(6), 538-578.

Erez, J. (2003). The source of ions for biomineralization in foraminifera and their implications for paleoceanographic proxies. Reviews in Mineralogy and Geochemistry, 54, 115–149.

Gründlingh, M. L. (1985). Occurrence of Red Sea Water in the southwestern Indian Ocean, 1981. Journal of Physical Oceanography, 15, 207–212. https://doi.org/10.1175/1520-0485(1985)015<0207:OORSWI>2.0.CO;2

Sen Gupta, B. K. (1989). Morphology and generic placement of the foraminifer 'Anomalina' wuellerstorfi Schwager. Journal of Paleontology, 63(5), 706–713. http://www.jstor.org/stable/1305636

Sen Gupta, B. K. (1984). Late Quaternary benthic foraminifera of the southern Norwegian Sea. In H. J. Oertli (Ed.), Benthos '83: Second International Symposium on Benthic Foraminifera (pp. 551–555).

Gussone, N., Filipsson, H. L., & Kuhnert, H. (2016). Mg/Ca, Sr/Ca and Ca isotope ratios in benthonic foraminifers related to test structure, mineralogy and environmental controls. Geochimica et Cosmochimica Acta, 173, 142–159.

Hasenfratz, A. P., Martínez-García, A., Jaccard, S. L., Vance, D., Wälle, M., Greaves, M., & Haug, G. H. (2017). Determination of the Mg/Mn ratio in foraminiferal coatings: An approach to correct Mg/Ca temperatures for Mn-rich contaminant phases. Earth and Planetary Science Letters, 457, 335–347.

Healey, S. L., Thunell, R. C., & Corliss, B. H. (2008). The Mg/Ca-temperature relationship of benthic foraminiferal calcite: New core-top calibrations in the <4 °C temperature range. Earth and Planetary Science Letters, 272(3–4). https://doi.org/10.1016/j.epsl.2008.05.023

Herbert, T. D. (2014). Alkenone Paleotemperature Determinations. In Treatise on Geochemistry. Second Edition. Elsevier Ltd, 8.15, pp. 399–433.

Hintz, C. J., Shaw, T. J., Bernhard, J. M., Chandler, T. G., McCorkle, D. C., & Blanks, J. K. (2006). Trace/minor element:calcium ratios in cultured benthic foraminifera. Part II: Ontogenetic variation. Geochimica et Cosmochimica Acta, 70, 1964–1976.

Jung, S. J. A., Kroon, D., Ganssen, G., Peeters, F., and Ganeshram, R.: Enhanced Arabian Sea intermediate water flow during glacial North Atlantic cold phases, Earth and Planetary Science Letters, 280, 220-228, 10.1016/j.epsl.2009.01.037, 2009.

Key, R. M., Olsen, A., van Heuven, S., Lauvset, S. K., Velo, A., Lin, X., Schirnick, C., Kozyr, A., Tanhua, T., Hoppema, M., Jutterström, S., Steinfeldt, R., Jeansson, E., Ishii, M., Perez, F. F., & Suzuki, T. (2015). Global Ocean Data Analysis Project, Version 2 (GLODAPv2), ORNL/CDIAC-162, NDP-093. Carbon Dioxide Information Analysis Center, Oak Ridge National Laboratory, US Department of Energy, Oak Ridge, Tennessee. doi:10.3334/CDIAC/OTG.NDP093_GLODAPv2

Koltermann, K. P., Gouretski, V. V., & Jancke, K. (2011). Hydrographic Atlas of the World Ocean Circulation Experiment (WOCE). In M. Sparrow, P. Chapman, & J. Gould (Eds.), Volume 3: Atlantic Ocean. International WOCE Project Office, Southampton, UK. ISBN 090417557X. https://doi.org/10.21976/C6RP4Z

Kroopnick, P. (1980). The distribution of ^13C in the Atlantic Ocean. Earth and Planetary Science Letters, 49, 469–484. https://doi.org/10.1016/0012-821X(80)90088-6

Lauvset, S. K., Lange, N., Tanhua, T., Bittig, H. C., Olsen, A., Kozyr, A., Alin, S., Alvarez, M., Azetsu-Scott, K., Barbero, L., Becker, S., Brown, P. J., Carter, B. R., da Cunha, L. C., Feely, R. A., Hoppema, M., Humphreys, M. P., Ishii, M., Jeansson, E., Jiang, L.-Q., Jones, S. D., Lo Monaco, C., Murata, A., Muller, J. D., Perez, F. F., Pfeil, B., Schirnick, C., Steinfeldt, R., Suzuki, T., Tilbrook, B., Ulfsbo, A., Velo, A., Woosley, R. J., and Key, R. M.: GLODAPv2.2022: the latest version of the global interior oceanbiogeochemical data product, Earth system science data, 14, 5543-5572, 10.5194/essd-14-5543-2022, 2022.~~Lauvset, S. K., Lange, N., Tanhua, T., Bittig, H. C., Olsen, A. C., Kozyr, A., ... Key, R. M. (2022). GLODAPv2.2022: the latest version of the global interior ocean biogeochemical data product. Earth System Science Data, submitted.~~

Lauvset, S. K., Lange, N., Tanhua, T., Bittig, H. C., Olsen, A., Kozyr, A., Álvarez, M., Azetsu-Scott, K., Brown, P. J., Carter, B. R., Cotrim da Cunha, L., Hoppema, M., Humphreys, M. P., Ishii, M., Jeansson, E., Murata, A., Müller, J. D., Pérez, F. F., Schirnick, C., Steinfeldt, R., Suzuki, T., Ulfsbo, A., Velo, A., Woosley, R. J., and Key, R. M.: The annual update GLODAPv2.2023: the global interior ocean biogeochemical data product, Earth Syst. Sci. Data, 16, 2047-2072, 10.5194/essd-16-2047-2024, 2024.

Lea, D., Mashiotta, T. A., & Spero, H. J. (1999). Controls on magnesium and strontium uptake in planktonic foraminifera determined by live culturing. Geochimica et Cosmochimica Acta, 63(16), 2369-2379.

Lear, C. H., Rosenthal, Y., & Slowey, N. (2002). Benthic foraminiferal Mg/ Ca paleothermometry: a revised core-top calibration. Geochimica et Cosmochimica Acta, 66(19), 3375–3387.

Lutze, G. F., & Thiel, H. (1989). Epibenthic foraminifera from elevated microhabitats; Cibicidoides wuellerstorfi and Planulina ariminensis. Journal of Foraminiferal Research, 19, 153-158. doi:10.2113/gsjfr.19.2.153

Lynch-Stieglitz, J., & Fairbanks, R. G. (1994). A conservative tracer for glacial ocean circulation from carbon isotope and paleo-nutrient measurements in benthic foraminifera. Nature, 369, 308–310. https://doi.org/10.1038/369308a0.

Martin, P. A., & Lea, D. W. (2002). A simple evaluation of cleaning procedures on fossil benthic foraminiferal Mg/Ca. Geochemistry, Geophysics, Geosystems, 3(10), 8401. doi:10.1029/2001GC000280.

Maxwell, J. L. (2019). Deep and Intermediate Water Mass History of the Western Indian Ocean. Dissertation, The University of Edinburgh.

McCave, I. N., Kiefer, T., Thornalley, D. J. R., & Elderfield, H. (2005). Deep flow in the Madagascar–Mascarene Basin over the last 150,000 years. Philosophical Transactions of the Royal Society of London. Series A: Mathematical, Physical, and Engineering Sciences, 363, 81–99.

Mekik, F., Noll, N., & Russo, M. (2010). Progress toward a multi-basin calibration for quantifying deep-sea calcite preservation in the tropical/subtropical world ocean. Earth and Planetary Science Letters, 299, 104-117.

Ni, S., Quintana Krupinski, N. B., Groeneveld, J., Persson, P., Somogyi, A., Brinkmann, I., Knudsen, K. L., Seidenkrantz, M.-S., & Filipsson, H. L. (2020). Early diagenesis of foraminiferal calcite under anoxic conditions: A case study from the Landsort Deep, Baltic Sea (IODP Site M0063). Chemical Geology. Advance online publication. https://doi.org/10.1016/j.chemgeo.2020.119871

Nuernberg, D. (1995). Magnesium in tests of Neogloboquadrina pachyderma sinistral from high northern and southern latitudes. Journal of Foraminiferal Research, 25, 350-368. doi:10.2113/gsjfr.25.4.350

Nuernberg, D., Bijma, J., & Hemleben, C. (1996). Assessing the reliability of magnesium in foraminiferal calcite as a proxy for water mass temperatures. Geochimica et Cosmochimica Acta, 60, 803-814. doi:10.1016/0016-7037(95)00446-7

Olsen, A., Key, R. M., van Heuven, S., Lauvset, S. K., Velo, A., Lin, X., Schirnick, C., Kozyr, A., Tanhua, T., Hoppema, M., Jutterström, S., Steinfeldt, R., Jeansson, E., Ishii, M., Pérez, F. F., & Suzuki, T. (2016). The Global Ocean Data Analysis Project version 2 (GLODAPv2) – an internally consistent data product for the world ocean. Earth System Science Data, 8, 297–323. doi:10.5194/essd-8-297-2016

Oppo, D. W., & Fairbanks, R. G. (1990). Atlantic Ocean thermohaline circulation of the last 150,000 years: Relationship to climate and atmospheric CO2. Paleoceanography, 5, 277–288. https://doi.org/10.1029/pa005i003p00277

Orsi, A. H., & Whitworth III, T. (2005). Hydrographic Atlas of the World Ocean Circulation Experiment (WOCE). Volume 1: Southern Ocean (Eds. M. Sparrow, P. Chapman, & J. Gould). International WOCE Project Office. https://doi.org/10.21976/C6BC78

Peña, L. D., Cacho, I., Calvo, E., Pelejero, C., Eggins, S., & Sadekov, A. (2008). Characterization of contaminant phases in foraminifera carbonates by electron microprobe mapping. Geochemistry, Geophysics, Geosystems, 9, Q07012. https://doi.org/10.1029/2008GC002018

Rathburn, A. E., & DeDeckker, P. (1997). Magnesium and strontium compositions of Recent benthic foraminifera from the Coral Sea, Australia and Prydz Bay, Antarctica. Marine Micropaleontology, 32, 231–248.

Ronge, T. A., Thomas A., Steph, S., Tiedemann, R., Prange, M., Merkel, U., Nürnberg, D., & Kuhn, G. (2015). Pushing the boundaries: Glacial/interglacial variability of intermediate and deep waters in the southwest Pacific over the last 350,000 years. Paleoceanography, 30(2), 23–38.

Rosenthal, Y., Boyle, E. A., Labeyrie, L., & Oppo, D. (1995). Glacial enrichments of authigenic Cd And U in subantarctic sediments: A climatic control on the elements' oceanic budget? Paleoceanography, 10, 395-413. doi:10.1029/95PA00310

Rosenthal, Y., Boyle, E., & Slowey, N. (1997). Temperature control on the incorporation of magnesium, strontium, fluorine and cadmium into benthic foraminiferal shells from Little Bahama Bank: prospects for thermocline paleoceanography. Geochimica et Cosmochimica Acta, 61(17), 3633–3643.

Rustic, G. T., Polissar, P. J., Ravelo, A. C., and DeMenocal, P.: Relationship between individual chamber and whole shell Mg/Ca ratios in Trilobatus sacculifer and implications for individual foraminifera palaeoceanographic reconstructions, Sci Rep, 11, 463, 10.1038/s41598-020-80673-8, 2021.

Sabine, C. L., Feely, R. A., Gruber, N., & Key, R. M. (2004). The oceanic sink for anthropogenic CO2. Science, 305(5682), 367-371.

Sadekov, A., Eggins, S. M., De Deckker, P., and Kroon, D.: Uncertainties in seawater thermometry deriving from intratest and intertest Mg/Ca variability in Globigerinoides ruber, Paleoceanography, 23, https://doi.org/10.1029/2007PA001452, 2008.

Saher, M. H., Rostek, F., Jung, S. J. A., Bard, E., Schneider, R. R., Greaves, M., Ganssen, G. M., Elderfield, H., & Kroon, D. (2009). Western Arabian Sea SST during the penultimate interglacial: A comparison of U37K′ and Mg/Ca paleothermometry. Paleoceanography, 24, PA2212. https://doi.org/10.1029/2007PA001557.

Sarnthein, M., Winn, K., Jung, S. J. A., Duplessy, J.-C., Labeyrie, L., Erlenkeuser, H., and Ganssen, G.: Changes in east Atlantic deepwater circulation over the last 30,000 years: Eight time slice reconstructions, Paleoceanography, 9, 209-267, 1994.

Schoenfeld, J. (2006). Taxonomy and distribution of the Uvigerina peregrina Plexus in the tropical to northeastern Atlantic. Journal of foraminiferal research, 36(4), 355–367.

Schwager, C. (1866). Fossile Foraminiferen von Kar Nicobar. Reeise dr Osterreichischen Fregatte Novara um Erde in den Jahren 1857, 1858, 1859 unter den Befehlen dees Commodore B. Von Willeerstorf-Urbair, Gologischer Thil, Vol. 2, No. 1. Geologische Beobachtungen, No. 2, Poläontologische Mittheilungen.

Schmidt, C., Hensen, C., Wallmann, K., Liebetrau, V., Tatzel, M., Schurr, S. L., Kutterolf, S., Haffert, L., Geilert, S., Hübscher, C., Lebas, E., Heuser, A., Schmidt, M., Strauss, H., Vogl, J., & Hansteen, T. (2019). Origin of High Mg and SO4 Fluids in Sediments of the Terceira Rift, Azores-Indications for Caminite Dissolution in a Waning Hydrothermal System. Geochemistry, geophysics, geosystems : G3, 20(12), 6078–6094.

Schweizer, M. (2006). Evolution and molecular phylogeny of Cibicides and Uvigerina (Rotaliida, foraminifera). Geologica Ultraiectina, 261, 1–167.

Schweizer, M., Pawlowski, J., Kouwenhoven, T., & van der Zwaan, B. (2009). Molecular phylogeny of common Cibicids and related Rotaliida (foraminifera) based on small subunit rDNA sequences. Journal of Foraminiferal Research, 39(4), 300–315.

Shackleton, N. (1967). Oxygen Isotope Analyses and Pleistocene Temperatures Re-assessed. Nature (London), 215, 15–17. https://doi.org/10.1038/215015a0.

Srinivasan, A. (1999). Deep circulation in the Indian Ocean: Tracer diagnostics, PhD

thesis, ProQuest Dissertations Publishing.

Spero, H. J., & Lea, D. W. (2002). The Cause of Carbon Isotope Minimum Events on Glacial Terminations. Science (American Association for the Advancement of Science), 296, 522–525.

Stirpe, C. R., Allen, K. A., Sikes, E. L., Zhou, X., Rosenthal, Y., Cruz-Uribe, A. M., & Brooks, H. L. (2021). The Mg/Ca proxy for temperature: A Uvigerina core-top study in the Southwest Pacific. Geochimica et cosmochimica acta, 309, 299–312.

Talley, L. D. (1999). Some aspects of ocean heat transport by the shallow, intermediate and deep overturning circulations. In Mechanisms of Global Climate Change at Millennial Time Scales, Geophys. Mono. Ser., 112, American Geophysical Union, ed. Clark, Webb and Keigwin, 1-22.

Talley, L. D. (2008). Freshwater transport estimates and the global overturning circulation: Shallow, deep and throughflow components. Progress in oceanography, 78(4), 257–303.

Talley, L. D. (2013a). Hydrographic Atlas of the World Ocean Circulation Experiment (WOCE). Volume 4: Indian Ocean (eds. M. Sparrow, P. Chapman and J. Gould). International WOCE Project Office, Southampton, UK, ISBN 0904175588. Online version: http: https://doi.org/10.21976/C61595.

Toole, J. M., & Warren, B. A. (1993). A hydrographic section across the subtropical South Indian Ocean. Deep-Sea Res. I 40, 1973-2019.

van Aken, H. M., Ridderinkhof, H., & de Ruijter, W. P. (2004). North Atlantic deep water in the south-western Indian Ocean. Deep Sea Research Part I: Oceanographic Research Papers, 51(6), 755–776.

van der Lubbe, J. J. L., R. Tjallingii, M. A. Prins, G.-J. A. Brummer, S. J. A. Jung, D. Kroon, and R. R. Schneider (2014), Sedimentation patterns

off the Zambezi River over the last 20,000 years, Mar. Geol., 355, 189–201, doi:10.1016/j.margeo.2014.05.012.

van Hinte, J. E., van Weering, T. C. E., and Troelstra, S. R.: Tracing a seasonal upwelling: Report on two cruises of R.V. Tyro to the NW Indian Ocean in 1992 and 1993., 146, 1995.

Van Markhoven, F. P. C. M., Berggren, W. A., & Edwards, A. S. (1986). Cenozoic Cosmopolitan Deep-Water Benthic Foraminifera. Bulletin des Centres de Recherches Exploration-Production Eld-Aquitaine, Mem. 11, Pau, 421 p.

You, Y. (2000). Implications of the deep circulation and ventilation of the Indian Ocean on the renewal mechanism of North Atlantic Deep Water. Journal of Geophysical Research: Oceans, 105, 23895–23926.

Yu, J., & Elderfield, H. (2008). Mg/Ca in the benthic foraminifera Cibicidoides wuellerstorfi and Cibicidoides mundulus: Temperature versus carbonate ion saturation. Earth and Planetary Science Letters, 276(1), 129–139.

Appendix A

Mg/Ca ratios and contamination indicators

Table A1 Samples analysed in Experiment 1-3

Sample ID	Core sample	Size fraction (μm)	Specimens containing	Crushing method
Experiment 1				
1a	929, Section 13, 58-58.5 cm	250-355	25 *G. ruber*	Two glass slides
1b	929, Section 13, 58-58.5 cm	250-355	25 *G. ruber*	Two glass slides
1c~~b~~	929, Section 13, 58-58.5 cm	250-355	10 *G. ruber*	Two glass slides
1d~~c~~	929, Section 13, 57.5-58 cm	250-355	20 *G. ruber*	Metal pin glass slide
1e~~d~~	929, Section 13, 58-58.5 cm	250-355	10 *G. ruber*	Metal pin glass mortar
1f~~e~~	929, Section 13, 57.5-58 cm	250-355	13 *G. ruber*	Metal pin glass mortar
Experiment 2				
2a	929, Section 13, 29-29.5 cm*	250-355	20 *G. ruber*	Metal pin glass mortar
2b	929, Section 13, 29-29.5 cm*	250-355	20 *G. ruber*	Metal pin glass mortar
2c	929, Section 13, 29.5-30 cm*	250-355	20 *G. ruber*	2-3 s in ultrasound
2d	929, Section 13, 57.5-58 cm*	250-355	20 *G. ruber*	2-3 s in ultrasound
2e	929, Section 13, 58-58.5 cm*	250-355	20 *G. ruber*	Not crushed
2f	929, Section 13, 57.5-58 cm*	250-355	20 *G. ruber*	Not crushed
2g	929, Section 13, 57.5-58 cm*	250-355	20 *G. ruber*	Not crushed
2h	929, Section 13, 57.5-58 cm*	250-355	20 *G. ruber*	Not crushed
Experiment 3				
3a	929, Section 14, 12.5-13.5 cm*	250-355	20 *G. ruber*	Metal pin glass mortar
3b	929, Section 14, 17-17.5 cm*	250-355	20 *G. ruber*	Metal pin glass mortar
3c	929, Section 14, 105.5-106 cm	250-355	10 *G. ruber*	Metal pin glass mortar
3d	929, Section 13, 105.5-106 cm	250-355	50 *G. ruber*	Metal pin glass mortar
3e	929, Section 13, 105.5-106 cm	250-355	30 *G. ruber*	Metal pin glass mortar
3f	929, Section 13, 105.5-106 cm	250-355	20 *G. ruber*	Metal pin glass mortar
3g	PE303-13[B], CT, 0-1 cm	250 - >450	5 *C~~ib~~ibicidoides~~.~~ spp.*	Metal pin glass mortar
3h	PE303-17[A], CT, 0-1 cm	250 - 450	5 *C~~ib~~ibicidoides~~.~~ spp.*	Not crushed
3i	PE303-17[A], CT, 0-1 cm	250 - 450	10 *Uvigerina~~vi.~~ spp.*	Metal pin glass mortar

*used for comparison to previously measured Mg/Ca ratios by Saher et al. (2009)

Table A2 Results from Experiment 1

Sample ID	Species	Mg/Ca (mmol/mol)	Fe/Ca (mmol/mol)	Al/Ca (mmol/mol)	Crushing technique[a]	Ca (ppm)	Specimens	Normalised Ca[b] (ppm/25 specimens)
1a	*G. ruber*	35.23	<LOD	<LOD	plate	0.55	25	0.55
1b	*G. ruber*	3.89	<LOD	<LOD	plate	7.50	25	7.50
1c	*G. ruber*	5.18	<LOD	<LOD	plate	3.75	10	9.37[b]
1d	*G. ruber*	5.84	<LOD	<LOD	pin	1.68	25	1.68
1e	*G. ruber*	4.54	<LOD	<LOD	pin	5.10	10	12.74[b]
1f	*G. ruber*	5.70	<LOD	<LOD	pin	5.66	10	14.16[b]

[b] Samples with specimens less than 25 have been normalised to account for the reduced sample in order to be able to compare effect of crushing technique on Ca content even though different sample size have been used (due to limited specimens available). Where 10 specimens have been analysed the Ca content have been multiplied with 2.5.

[a] plate = crushing specimens simultaneously between two glass plates, pin = crushing specimens individually using metal pin

Table A3~~2.~~ Results from Experiment 2~~1~~-3

Sample ID	Species	Mg/Ca (mmol/mol)	Fe/Ca (mmol/mol)	Al/Ca (mmol/mol)	Mn/Ca (mmol/mol)	Ca (ppm)	Note
2a	*G. ruber*	5.64	0.51	2.36	0.18	19.33	
2b	*G. ruber*	4.40	<LOD	3.80	0.15	7.92	
2c	*G. ruber*	4.66	0.18	1.84	0.17	22.54	
2d	*G. ruber*	6.58	0.78	3.61	0.20	13.99	
2e	*G. ruber*	4.71	0.27	1.67	0.15	30.16	
2f	*G. ruber*	5.49	<LOD	4.34	0.16	7.32	
2g	*G. ruber*	4.85	0.43	2.11	0.18	24.18	
2h	*G. ruber*	9.41	1.56	3.96	0.34	30.92	
3a	*G. ruber*	3.17	0.39	0.91	0.11	2.15	
3b	*G. ruber*	3.7	<LOD	<LOD	0.13	21.15	
3c	*G. ruber*	3.99	1.08	0.96	0.17	27.48	
3d	*G. ruber*	3.59	<LOD	0.87	0.15	11.27	
3e	*G. ruber*	4.48	0.56	1.61	0.18	88.35	

3f	*G. ruber*	3.78	0.39	5.93	0.14	31.66
3g	*Cibicidoides spp.~~G. ruber~~*	2.37	<LOD	3.36	0.17	35.39
3h	*Cibicidoides spp.~~G. ruber~~*	2.54	1.08	0.91	0.04	4.32
3i	*Uvigerina spp.~~G. ruber~~*	2.75	<LOD	<LOD	0.07	11.80

Table A4~~3~~. Mg/Ca, Ca and contamination indicators (Fe/Ca, Al/Ca and Mn/Ca) of samples containing *G. ruber* analysed in the same runs alongside core-top samples.

Core	Species	Mg/Ca	Fe/Ca	Al/Ca	Mn/Ca	Ca	Note*
NIOP929	*G. ruber*	3.70	0.14	0.36	0.17	17.82	*Cibicidoides~~.~~ spp.*
NIOP929	*G. ruber*	3.56	0.10	0.35	0.19	25.60	*Cibicidoides~~.~~ spp.*
NIOP929	*G. ruber*	3.17	0.09	0.31	0.12	28.36	*Cibicidoides spp.~~C. spp.~~*
NIOP929	*G. ruber*	3.16	0.23	<LOD	0.17	10.60	*Cibicidoides spp.~~C. spp.~~*
NIOP929	*G. ruber*	4.18	0.12	0.29	0.17	19.78	*Cibicidoides spp.~~C. spp.~~*
NIOP929	*G. ruber*	3.26	0.10	0.25	0.15	24.51	*Cibicidoides spp.~~C. spp.~~*
NIOP929	*G. ruber*	5.22	0.38	1.31	0.11	24.48	*U. peregrina*
NIOP929	*G. ruber*	4.77	0.24	0.92	0.14	50.88	*U. peregrina*
NIOP929	*G. ruber*	5.1	0.30	1.04	0.12	39.95	*U. peregrina*

*Analysed in run alongside *Cibicidoides~~.~~ spp./U. peregrina*

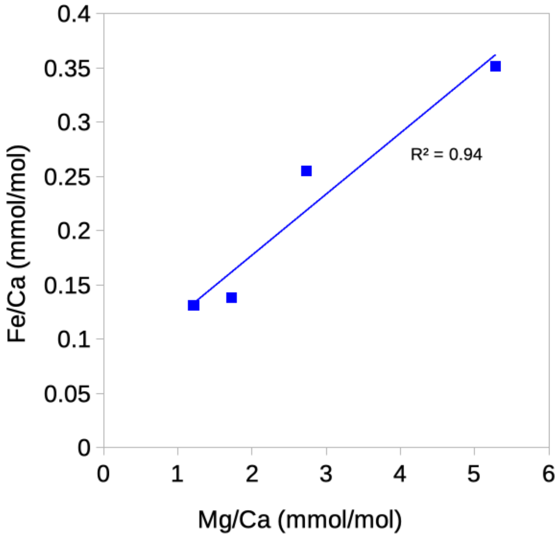

Figure~~.~~ A1 Correlation between Fe/Ca ratios and Mg/Ca ratios in *Cibicidoides wuellerestorfi*.~~.~~ One datapoint is excluded where Fe is below limit of detection.

Appendix B

ICP-OES calibration curves and standards

Table B1 Concentration of standards used (Mg in ppb and Ca in ppm) in Mg/Ca analysis for calibration and for matrix effect.

Tube	Sample Labels	Al 396.152 mg/L	Ca 315.887 mg/L	Ca 317.933 mg/L	Ca 422.673 mg/L	Mg 279.553 ug/L	Mg 280.270 ug/L	Mg 285.213 ug/L
1 : 1	UoE benthos Blank	0.000000	0.000000	0.000000	0.000000	0.000000	0.000000	0.000000
1 : 2	UoE benthos St1		13.8500	13.8500	13.8500	75.5000	75.5000	75.5000
1 : 3	UoE benthos St2		16.5000	16.5000	16.5000	258.000	258.000	258.000
1 : 4	UoE benthos St3		13.8500	13.8500	13.8500	339.000	339.000	339.000
1 : 5	UoE benthos St4		13.8500	13.8500	13.8500	466.000	466.000	466.000
1 : 6	UoE benthos St5		13.8500	13.8500	13.8500	677.000	677.000	677.000
1 : 7	UoE benthos St6		13.8500	13.8500	13.8500	1379.00	1379.00	1379.00
1 : 8	Standard 8							
1 : 9	Standard 9	0.500000	0.500000	0.500000	0.500000			
1 : 10	Standard 10	2.50000	2.50000	2.50000	2.50000			
1 : 11	Standard 11	10.0000	10.0000	10.0000	10.0000			
1 : 12	Standard 12	50.0000	50.0000	50.0000	50.0000			

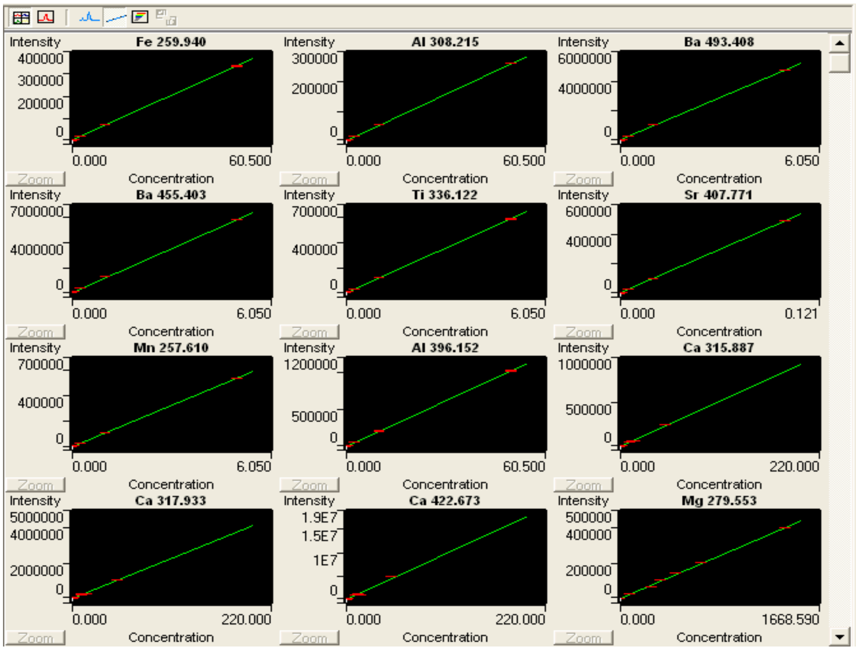

Fig<u>ure</u>~~.~~ B1. Print screen of ICP Expert showing calibration curves for standards in *Uvigerina peregrina* analysis

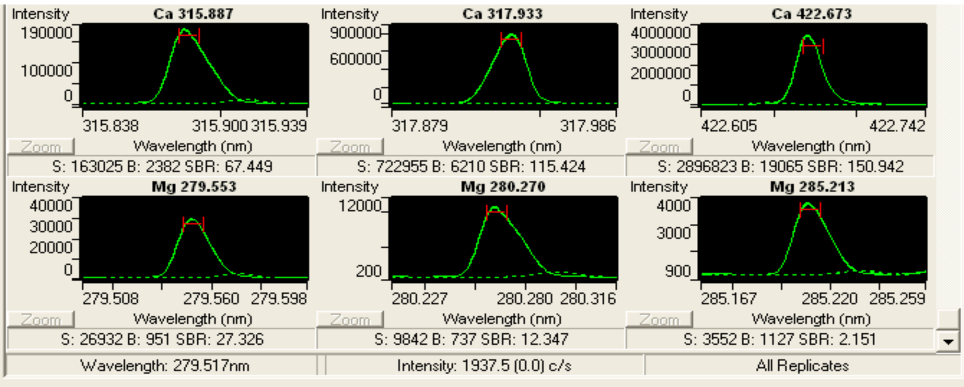

Fig<u>ure</u>~~.~~ B2. Print screen of ICP Expert showing intensity curves in *Cibicidoides spp*<u>.</u> analysis

Appendix C

Qualitative observations of benthic foraminifera samples analysed

Table 1C Images and qualitative observations of 250-450 µm size fractions of core top samples containing benthic foraminifera tests analysed.

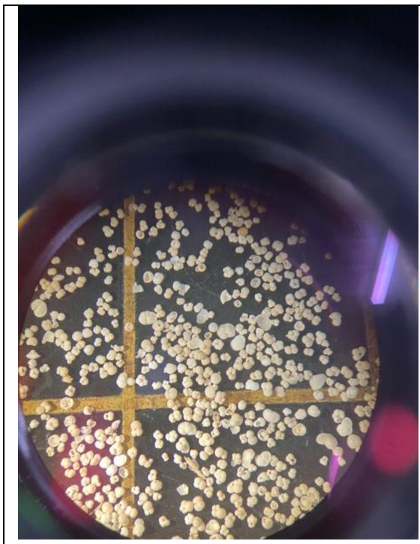	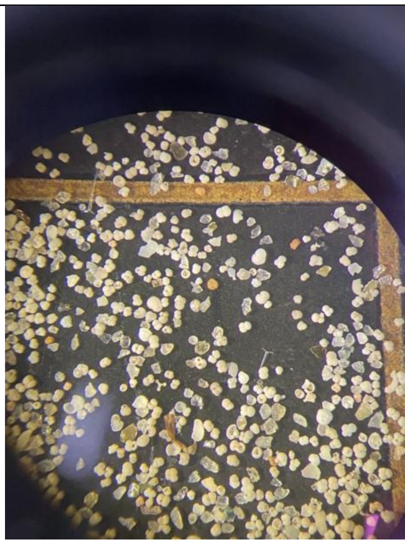	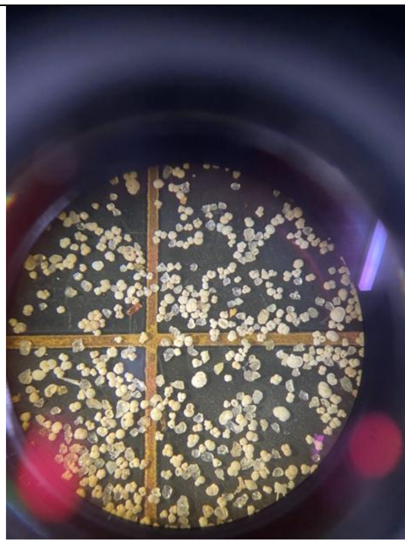
PE303-3	PE303-4c	PE303-6c
- no debris or quartz - clean - broken fragments present but most tests intact - mostly unstained/ minor discoloration - no sign of secondary calcification or corrosion	- 50% quartz - clean - tests mostly intact - mostly unstained/ minor discoloration - no sign of secondary calcification or corrosion	- 50% quartz - clean - tests mostly intact - mostly unstained/minor discoloration - no sign of secondary calcification or corrosion
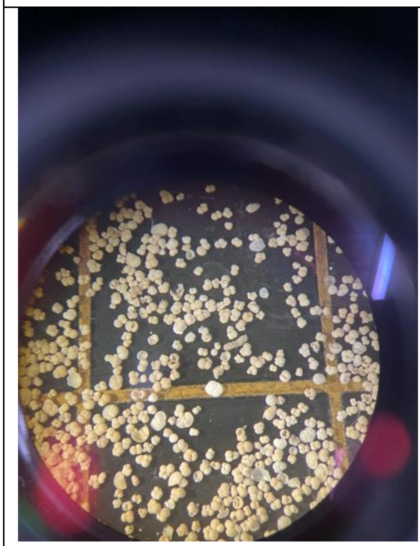	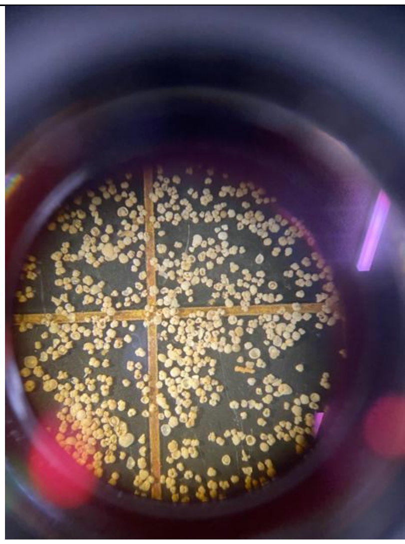	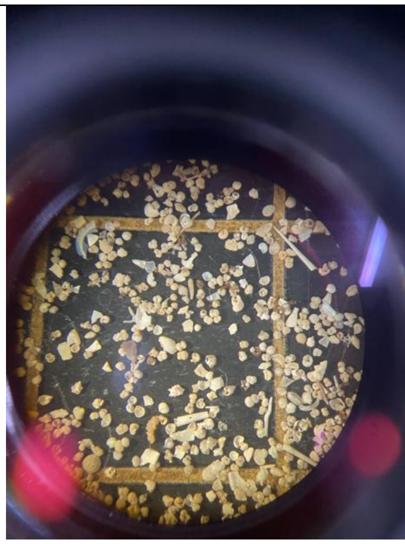
PE303-14a	PE303-17a	PE303-18b

- no debris or quartz - broken tests present but most intact - some signs of secondary calcification and corrosion white no discoloration	- no debris or quartz - mixed condition, visible mud on tests - discoloration and corrosion	- debris and quartz present - visible mud on tests - broken fragments - discoloration and corrosion present - no sign of secondary calcification
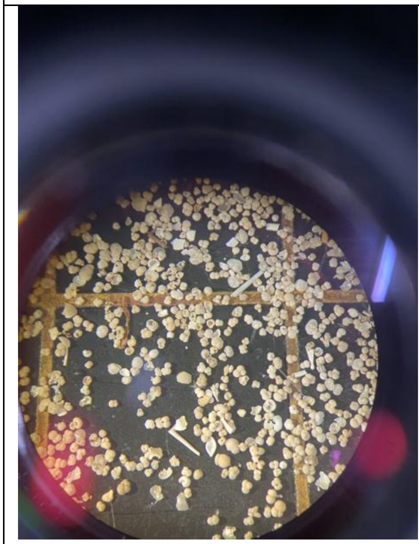	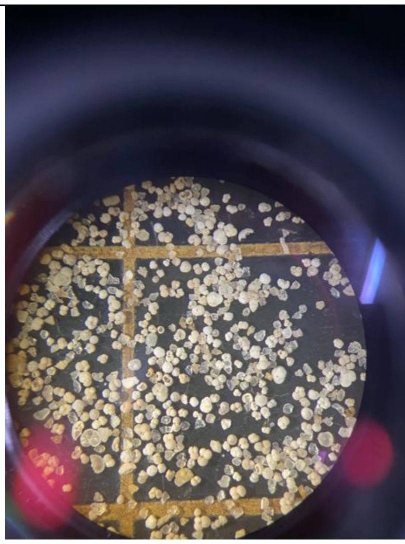	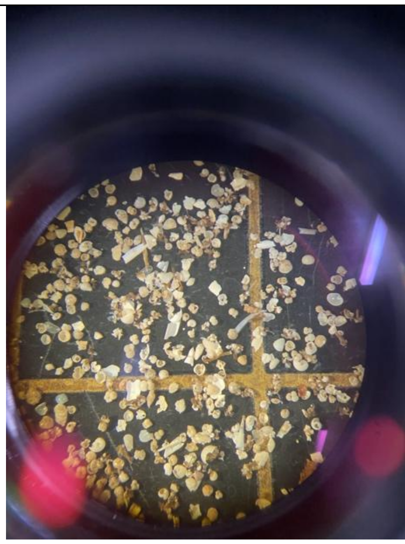
PE303-22	PE303-50	PE304-9
- debris present, no quartz - mixed condition, some discoloration corrosion and secondary calcification - broken fragments	- >50% quartz, no debris - clean - mixed condition, minor discoloration and some visible mud - some broken tests - minor corrosion - no sign of secondary calcification	- debris and quartz present - visible mud - broken fragments >50% - discoloration - corrosion - no sign of secondary calcification
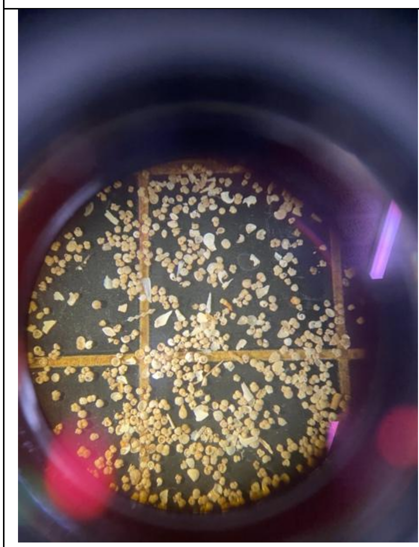	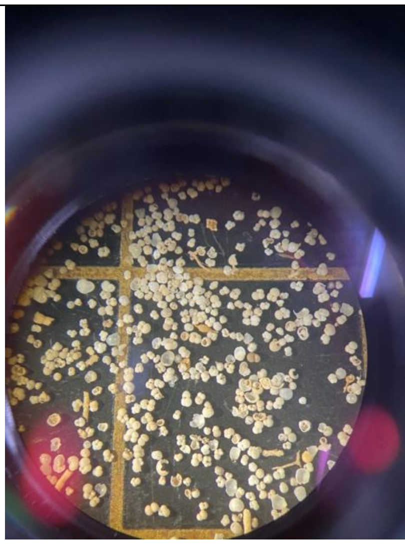	

PE304-25	PE304-30	
- no quartz or debris - most tests have visible mud - broken fragments - brown/orange discoloration - no visible sign of corrosion or secondary calcification	- no quartz or debris - mixed condition, some visible dirt - minor discoloration - broken test fragments - corrosion - minor secondary calcification	